TU Delft

Plant Skeleton Extraction and Stem-leaf Segmentation

October 30th, 2024

Qiwei Shen

1st supervisor: Liangliang Nan

2nd supervisor: Jantien Stoter

Co-reader: Roderik Lindenbergh

Delegate: Daniëlle Groetelaers

CONTENT

01 Introduction

02 Related Work

03 Methodology

04 Results & Discussion

05 Conclusion & Future Work

Introduction

Introduction

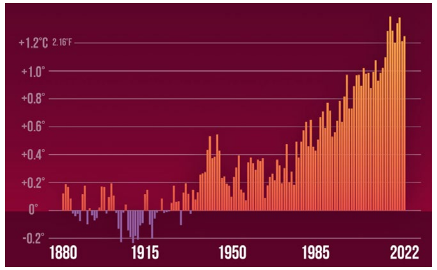

Climate change

Soil degradation

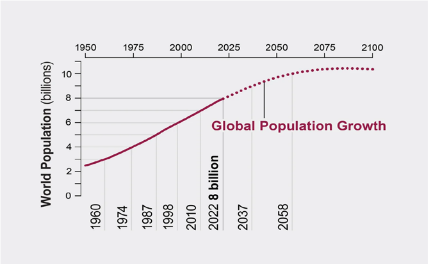

Global population growth

Food Shortage
& Security

Li et al., 2020; Liu et al., 2019; Panjvani et al., 2019; Xu et al., 2019.

Introduction

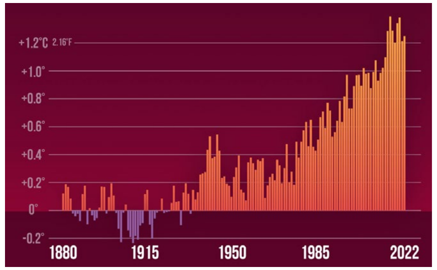

Climate change

Soil degradation

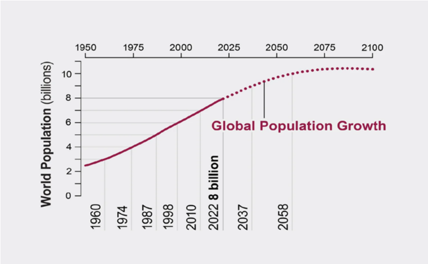

Global population growth

Food Shortage
& Security

- Environment-resilient
- High-quality
- High-production

Genetic Breeding

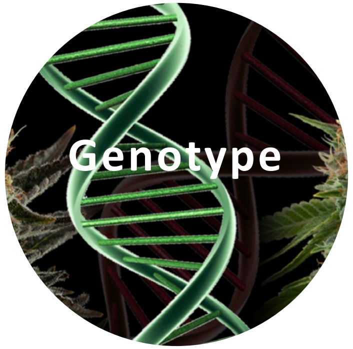

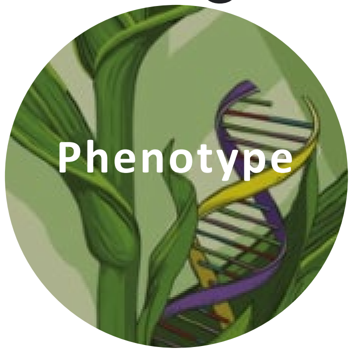

Linkage mapping

Li et al., 2020; Liu et al., 2019; Panjvani et al., 2019; Xu et al., 2019.

Introduction

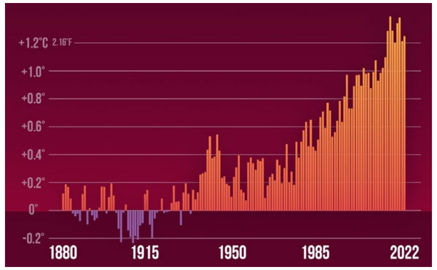

Climate change

Soil degradation

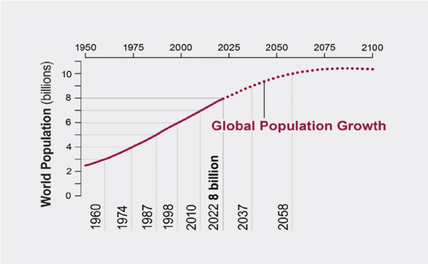

Global population growth

Food Shortage & Security

Genetic Breeding

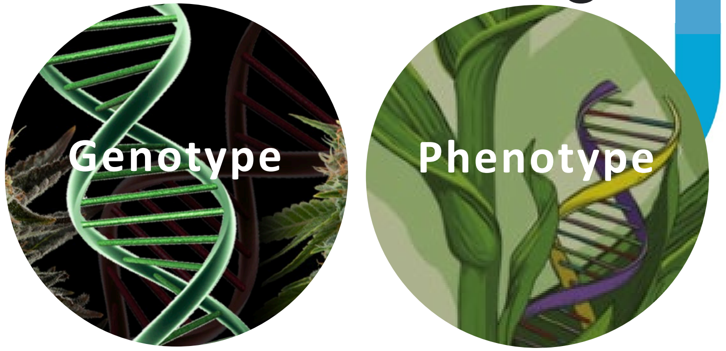

Linkage mapping

Plant Phenotyping

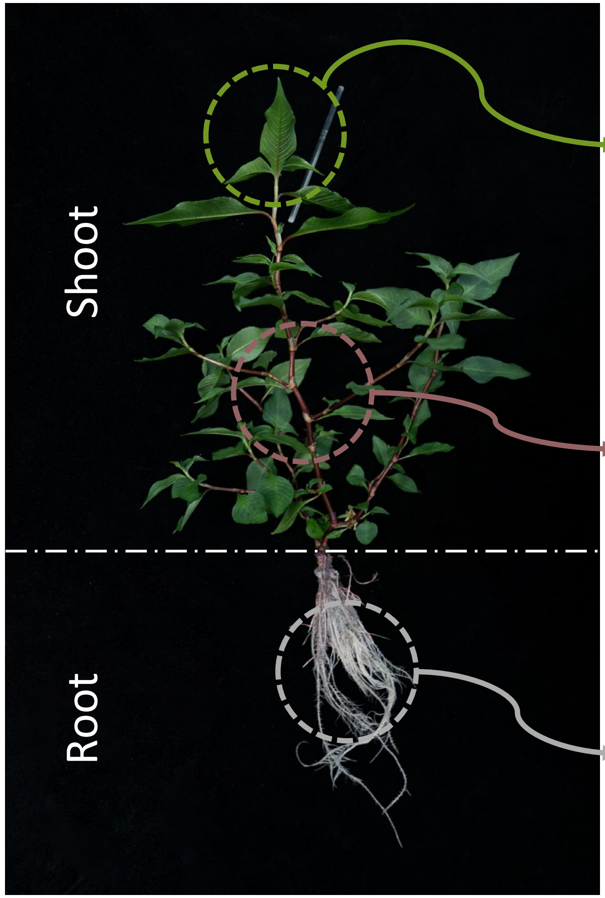

Leaf traits:
- Leaf area
- Leaf angles
- etc.

Stem traits:
- Stem length
- Stem width
- etc.

Root traits:
- Root structure
- etc.

Li et al., 2020; Liu et al., 2019; Panjvani et al., 2019; Xu et al., 2019.

Introduction

- ➢ Traditional phenotyping

 

Zhao et al., 2019; Harandi et al., 2023; Li et al., 2020.

Introduction

➢ Traditional phenotyping

 

- Labor-intensive
- Time-consuming
- Invasive

Phenotypic Bottleneck

Zhao et al., 2019; Harandi et al., 2023; Li et al., 2020.

Introduction

➢ Traditional phenotyping

- Labor-intensive
- Time-consuming
- Invasive

Phenotypic Bottleneck

3D phenotyping

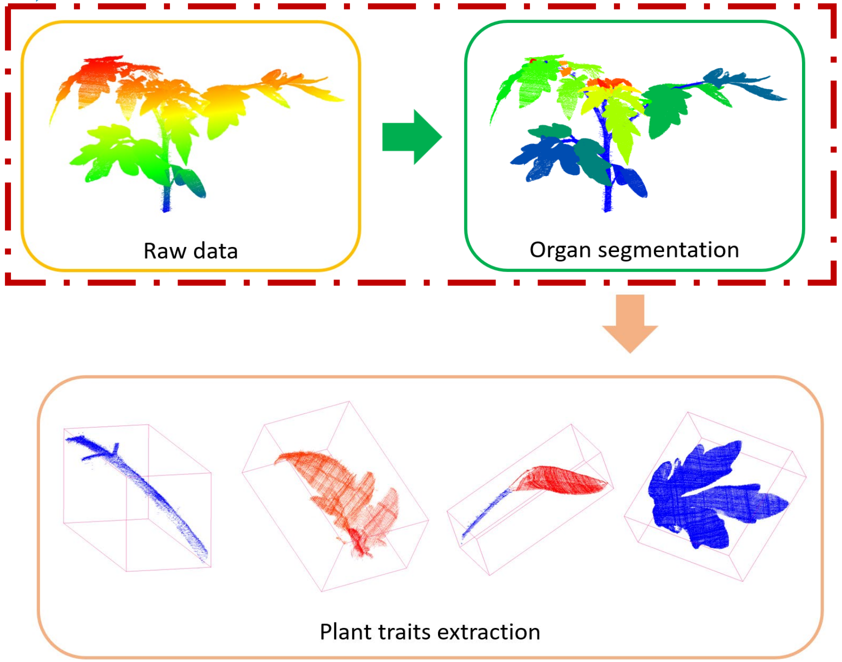

Zhao et al., 2019; Harandi et al., 2023; Li et al., 2020.

Introduction

➢ Traditional phenotyping

- Labor-intensive
- Time-consuming
- Invasive

Phenotypic Bottleneck

3D phenotyping

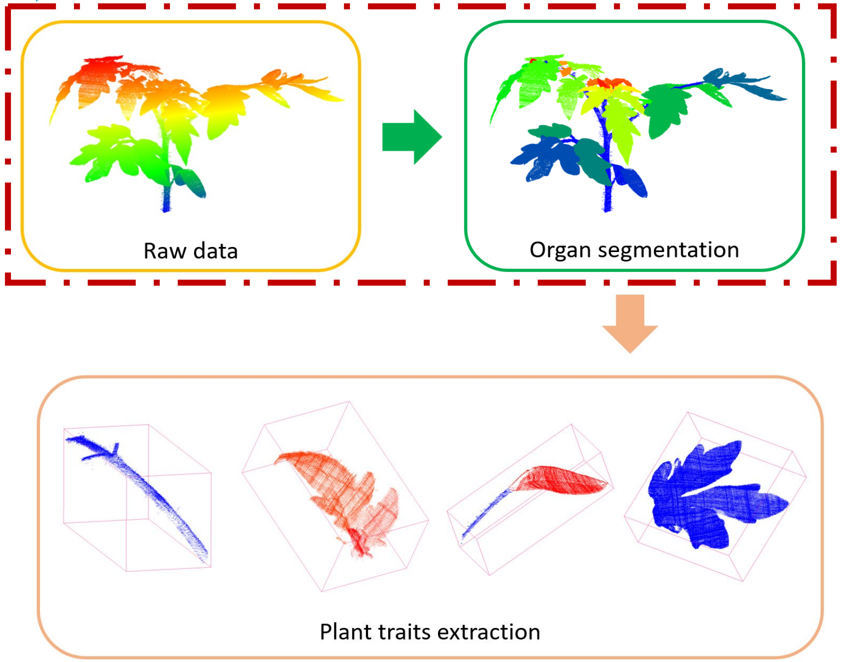

- Automatic
- High-precision
- Non-invasive
- High-throughput

Zhao et al., 2019; Harandi et al., 2023; Li et al., 2020.

Introduction - Plant Organ Segmentation

➢ Plant organ segmentation

- Skeleton-based approach

local features global features

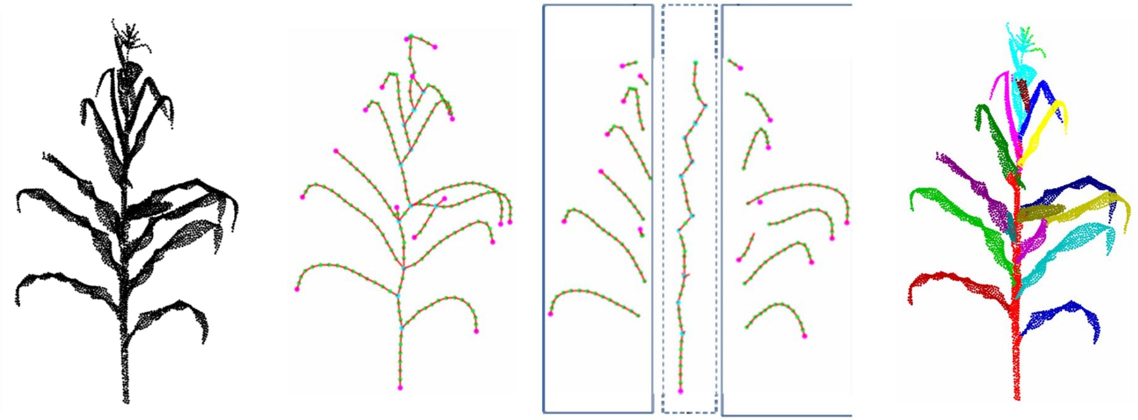

- Skeleton → Geometry and topology structure
- Plant skeleton → Plant organ instance segmentation

Cao et al., 2010; Ma et al., 2023.

Related Work

Related Work

➢ Slice clustering

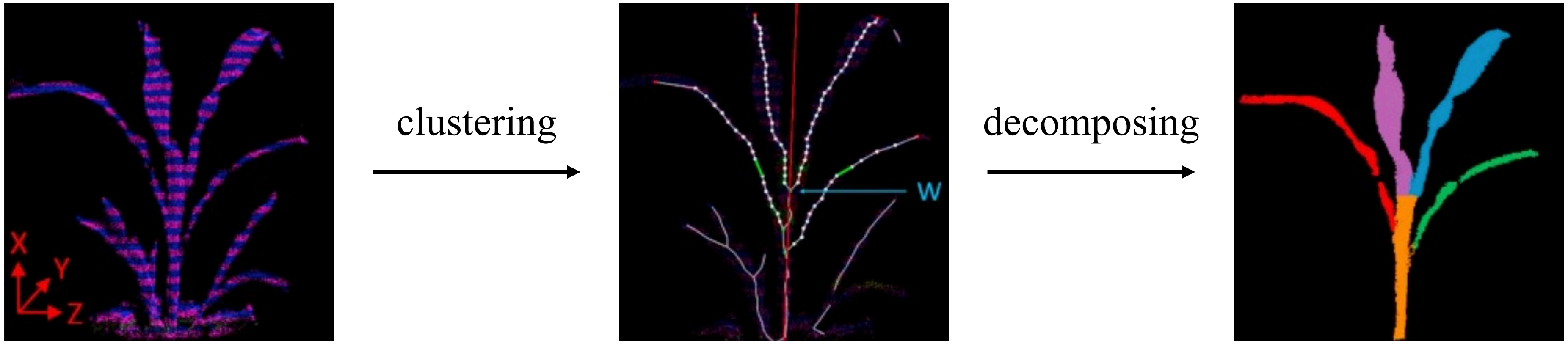

Sliced point cloud | Skeleton | Stem-leaf segmentation

Xiang et al., 2019.

Related Work

➢ Slice clustering

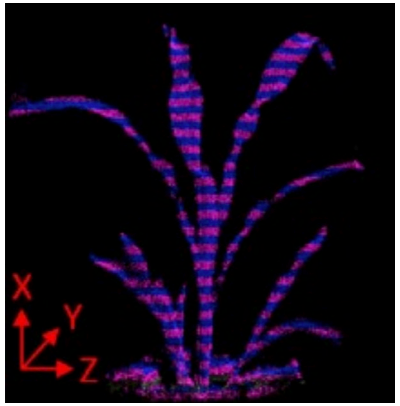

Sliced point cloud

clustering →

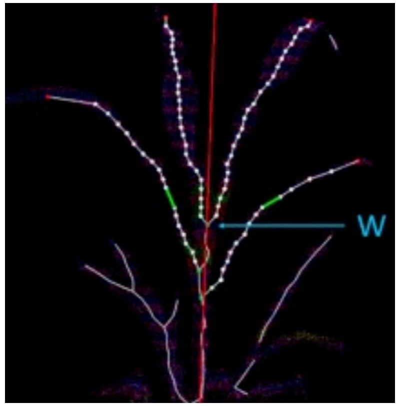

Skeleton

decomposing →

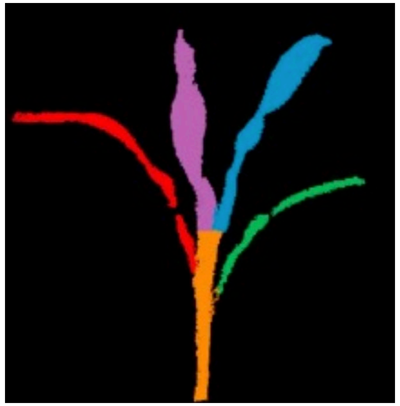

Stem-leaf segmentation

- Simple and intuitive;
- Horizontal parts of the plant are not well processed

Xiang et al., 2019.

Related Work

- L_1-medial skeleton algorithm

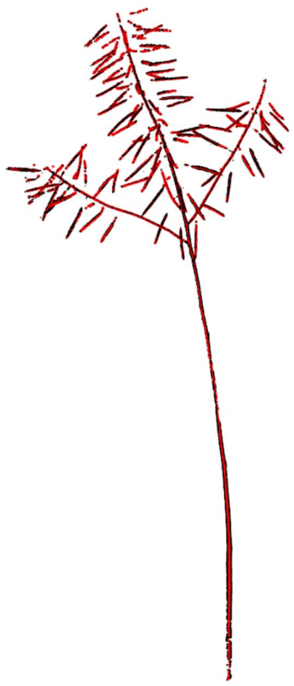

Oilseed rape skeleton

decomposing →

Recall: 92.23%

Silique instances

Ma et al., 2023.

Related Work

➢ L_1-medial skeleton algorithm

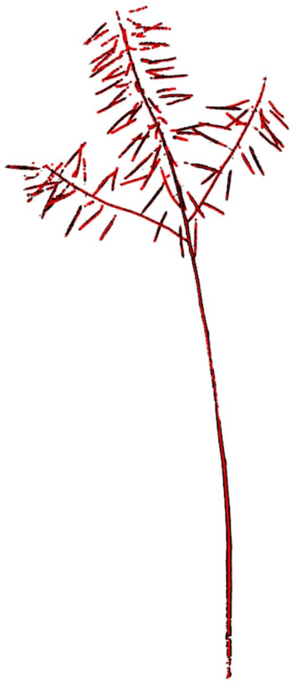

Oilseed rape skeleton

decomposing →

Recall: 92.23%

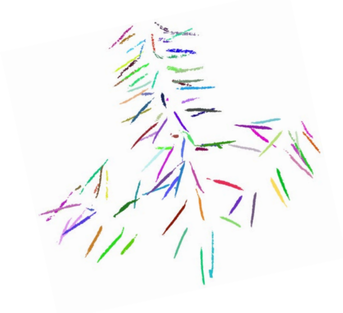

Silique instances

- Can handle complex cylindrical structures;
- Maintain the centeredness of skeleton.
- Not suitable for flat or planar structures, such as wide leaves.

Ma et al., 2023.

Related Work

➢ Laplacian-based contraction (LBC) algorithm

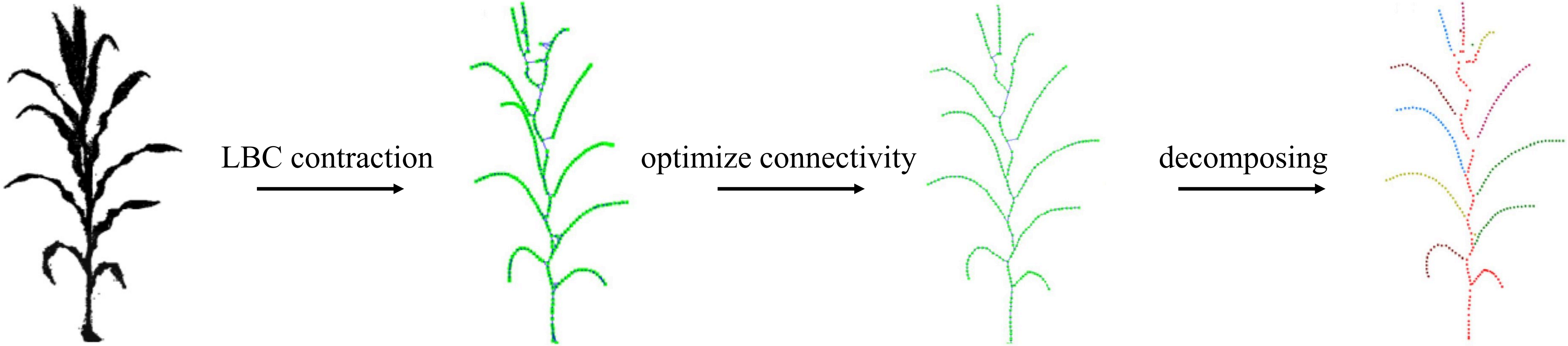

Original Point Cloud | Initial Skeleton | Optimized Skeleton | Skeleton decomposition

TU Delft

Wu et al., 2019.

Related Work

➢ Laplacian-based contraction (LBC) algorithm

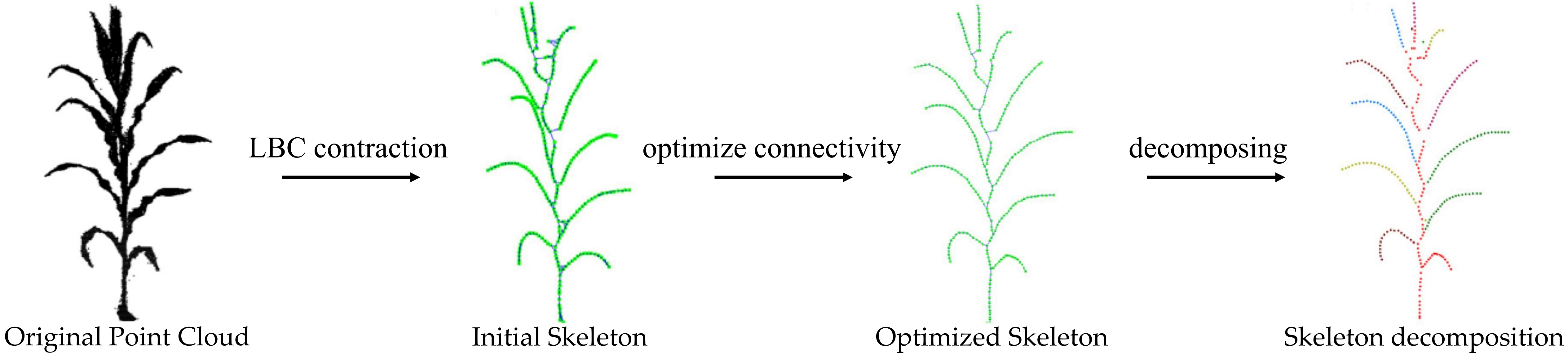

- Can contract plant stems and leaves into skeletal objects;
- Contain zigzag structures, abnormal branches often appear;
- Geometric constraints need to be incorporated.

Wu et al., 2019.

Related Work

➢ AdTree

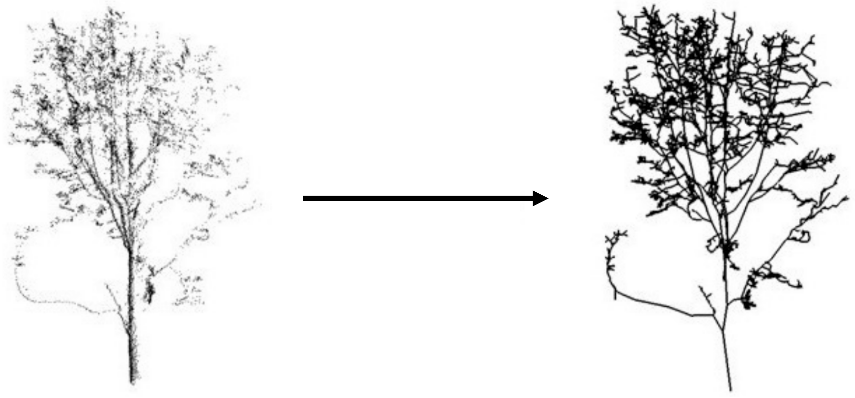

➢ WoodSKE

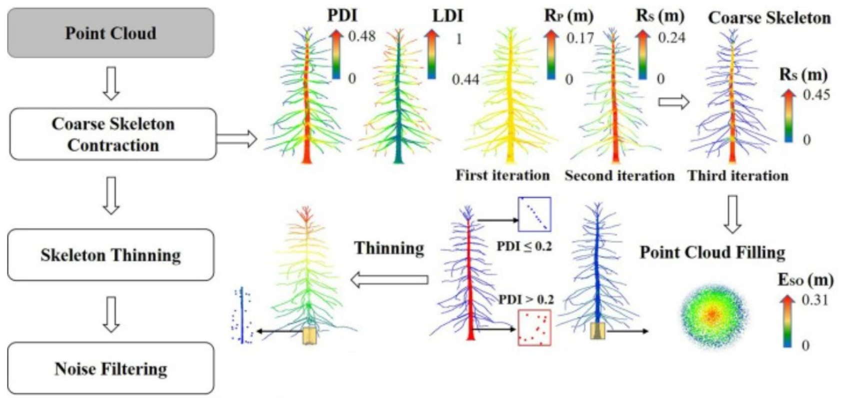

Du et al., 2019; Wu et al., 2021.

Related Work

➢ AdTree

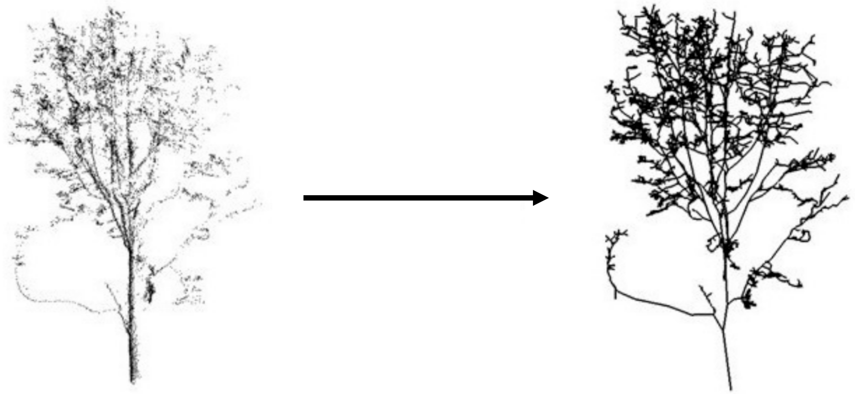

➢ WoodSKE

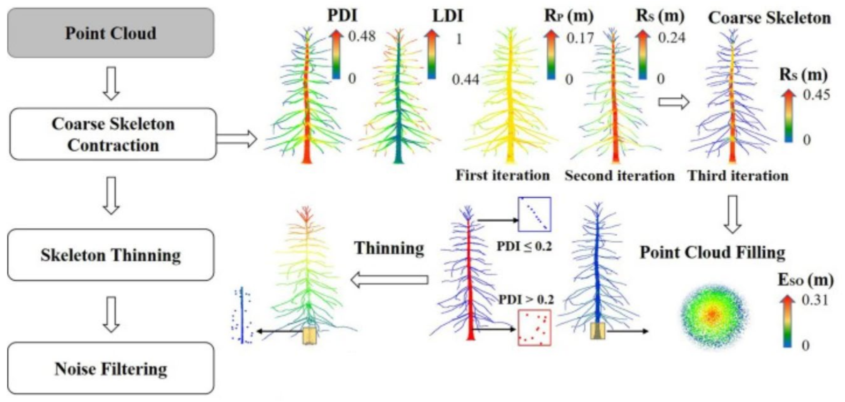

- Can efficiently extract the skeletons of tree branches;
- Do not adequately address the skeleton extraction of plant leaves.

Du et al., 2019; Wu et al., 2021.

Research Gap & Objectives

➢ Limitations of previous studies

- Often struggle with plant leaves;
- Poorly in mitigating zigzag structures, preserving fine details, and maintaining centrality.

➢ Target plants are simple

- With a single main stem, few or no lateral stems, and minimal or no leaves.

➢ A framework that integrates plant skeletonization and stem-leaf segmentation

- Extracting curve skeletons from **leafy plant (herbaceous plant)** point clouds
- Establishing stem-leaf segmentation based on extracted curve skeleton

Methodology

Methodology - Overview

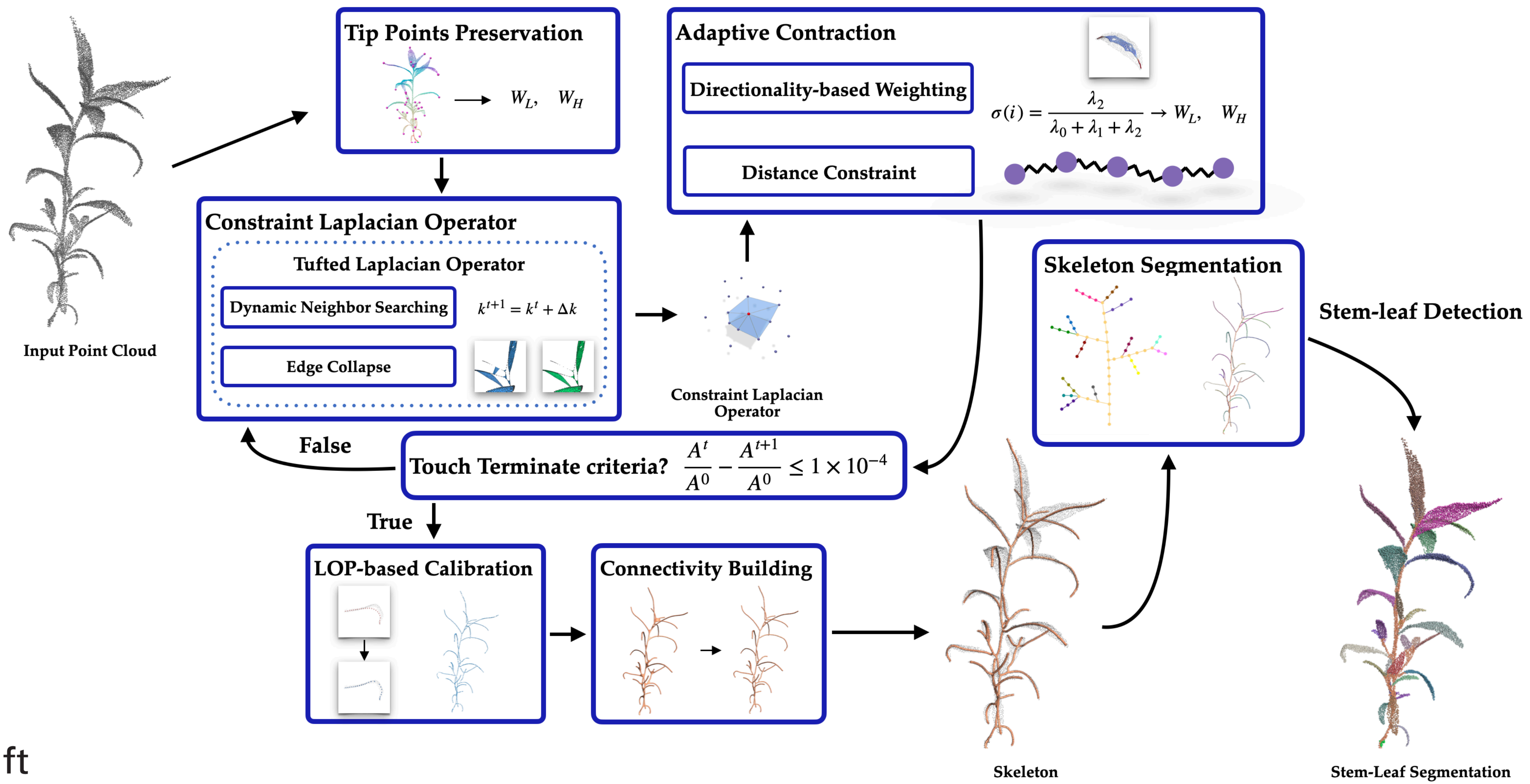

TU Delft

Methodology - Point Cloud Contraction

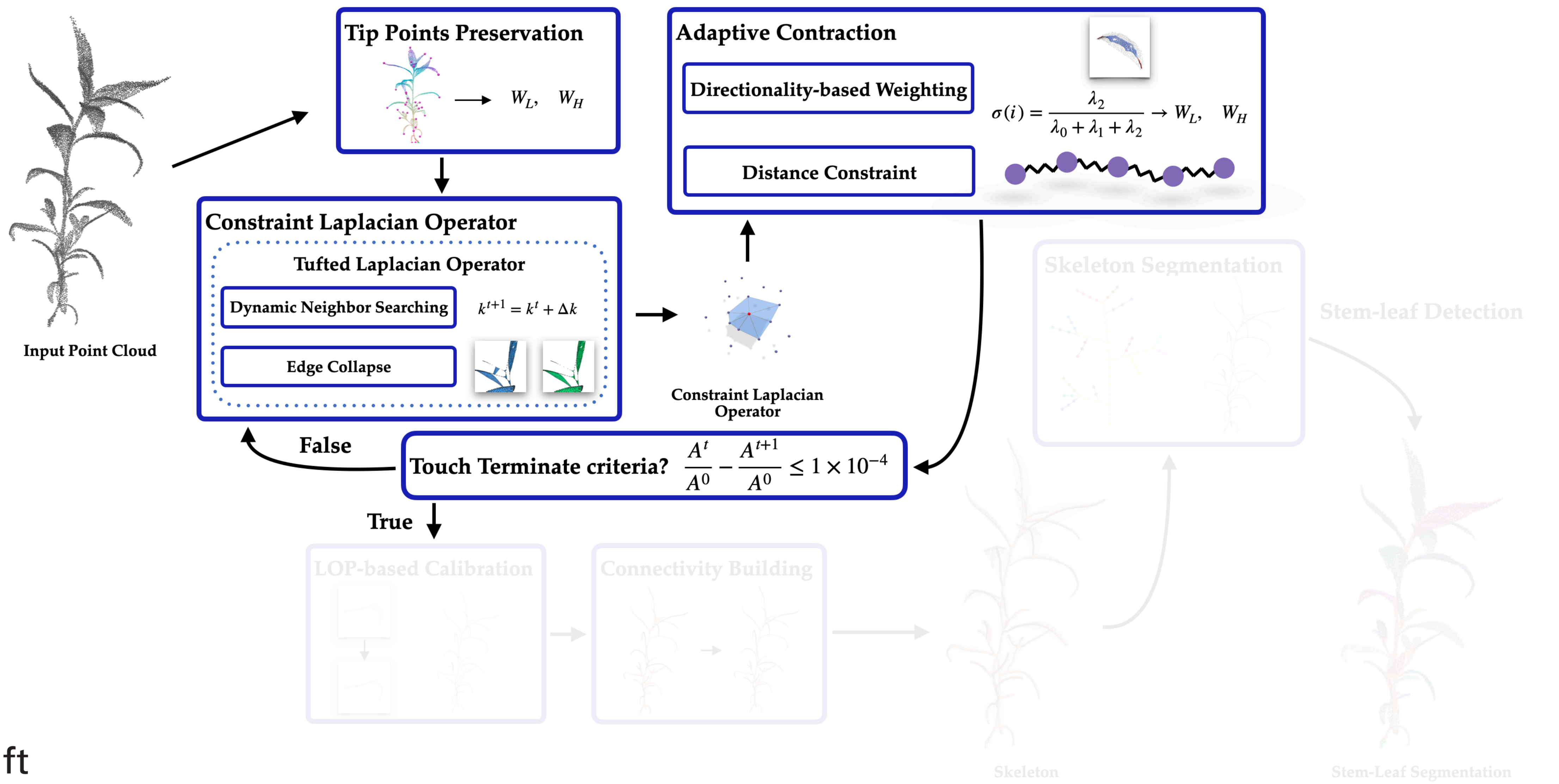

Methodology - Skeleton Graph Generation

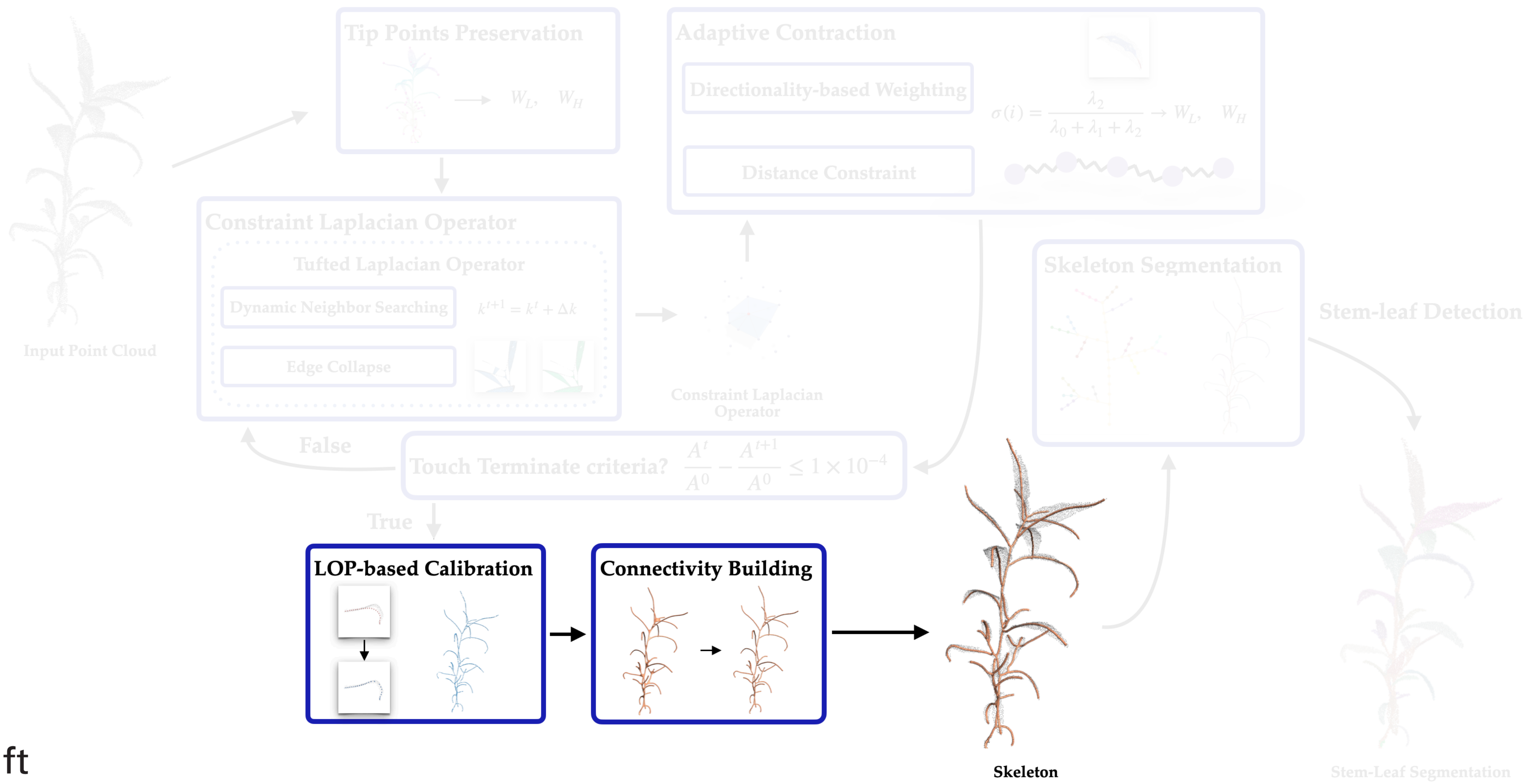

Methodology - Stem-Leaf Segmentation

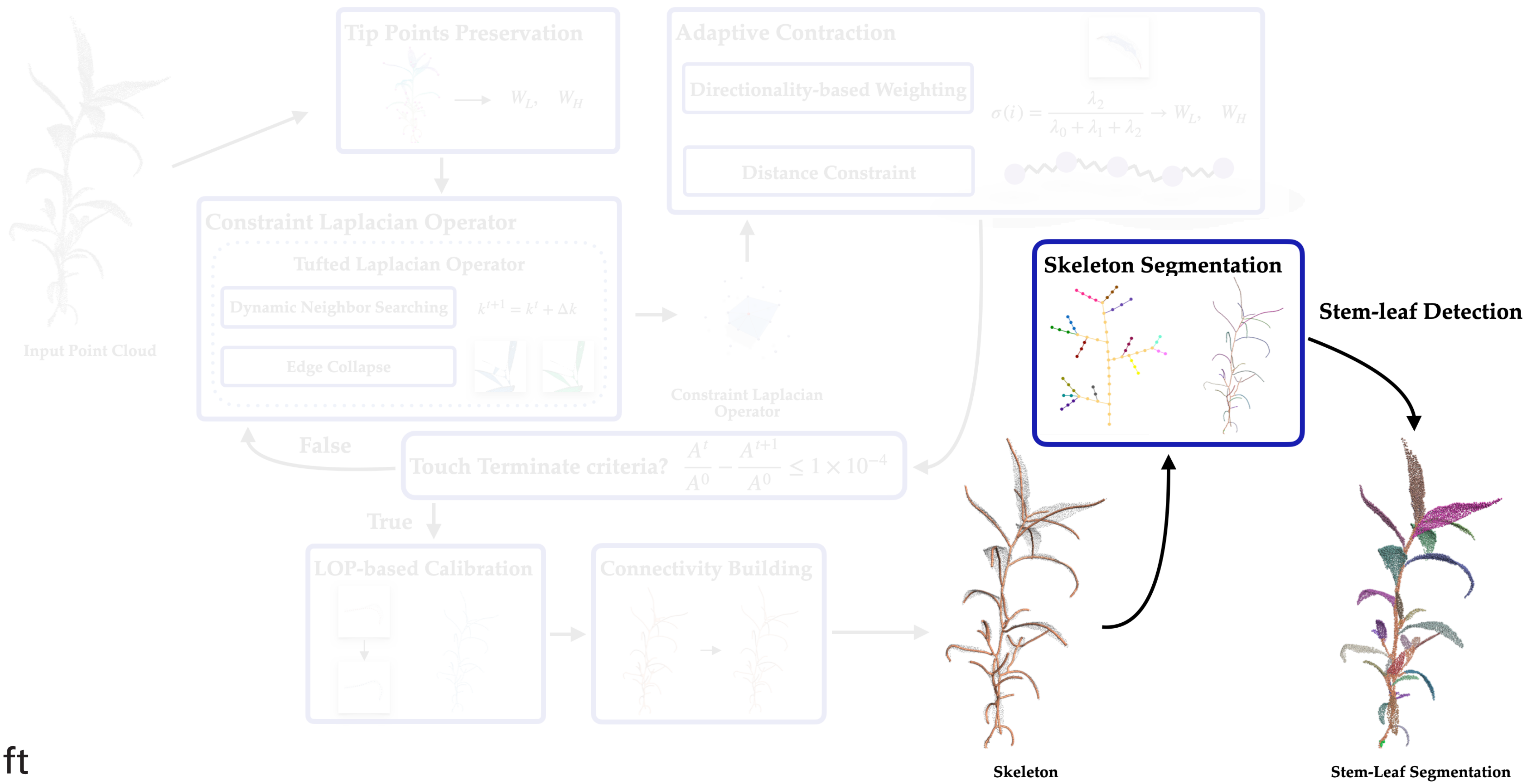

Methodology - Point Cloud Contraction

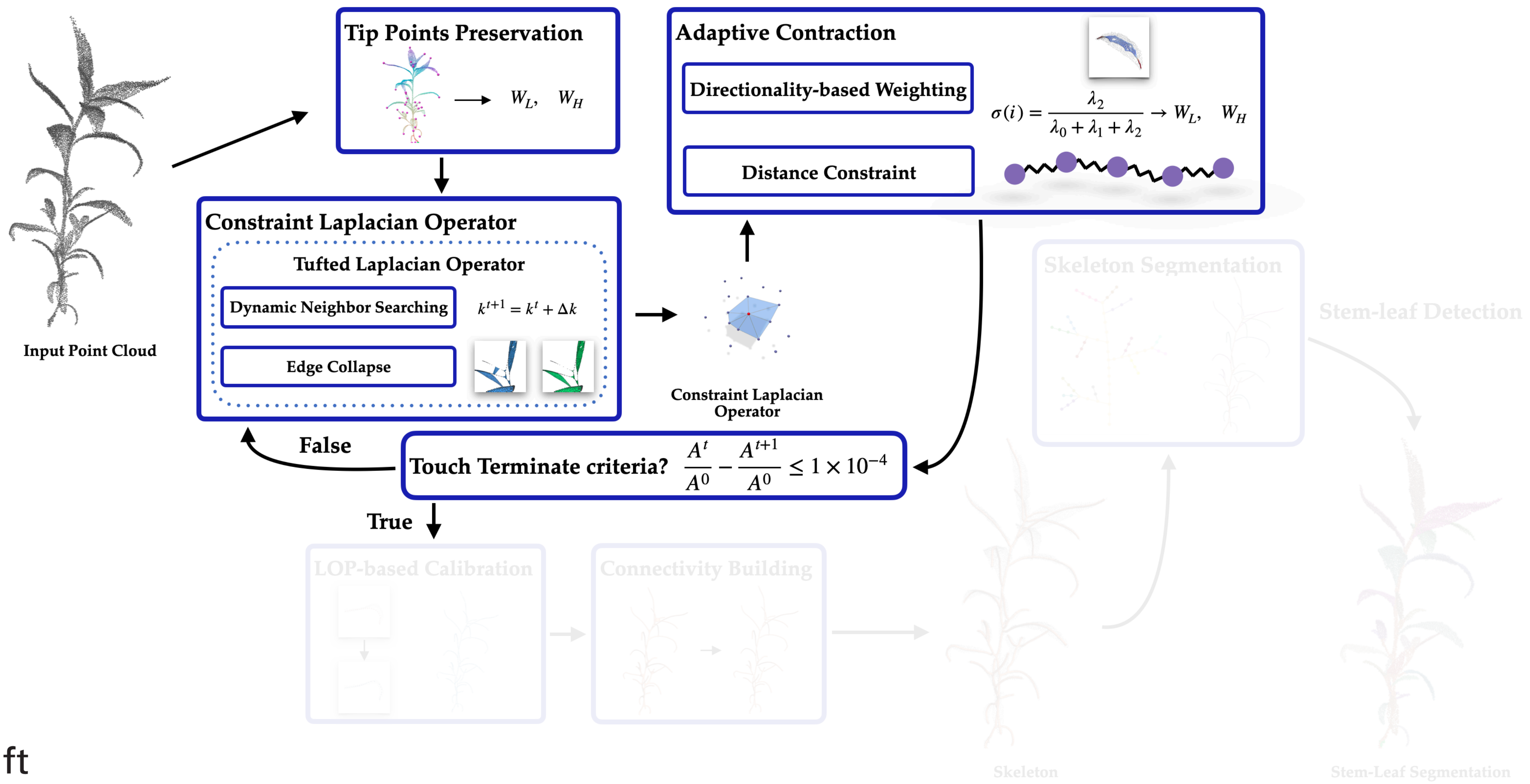

Methodology - Point Cloud Contraction

➢ Overview of LBC algorithm

- Moving the vertices along their approximate mean curvature normal directions (approximated by cotangent-weighted Laplacian operator L);
- Solving the linear system iteratively: $\begin{bmatrix} \mathbf{W}_L L \\ \mathbf{W}_H \end{bmatrix} \mathbf{P}^{t+1} = \begin{bmatrix} 0 \\ \mathbf{W}_H \mathbf{P}^t \end{bmatrix}$

Cao et al., 2010.

Methodology - Point Cloud Contraction

➢ Overview of LBC algorithm

Discrete skeleton points

Methodology - Point Cloud Contraction

➢ Overview of LBC algorithm

Discrete skeleton points

Skeleton

Methodology - Point Cloud Contraction

➢ Overview of LBC algorithm

- Drawbacks of the contracted discrete skeleton points

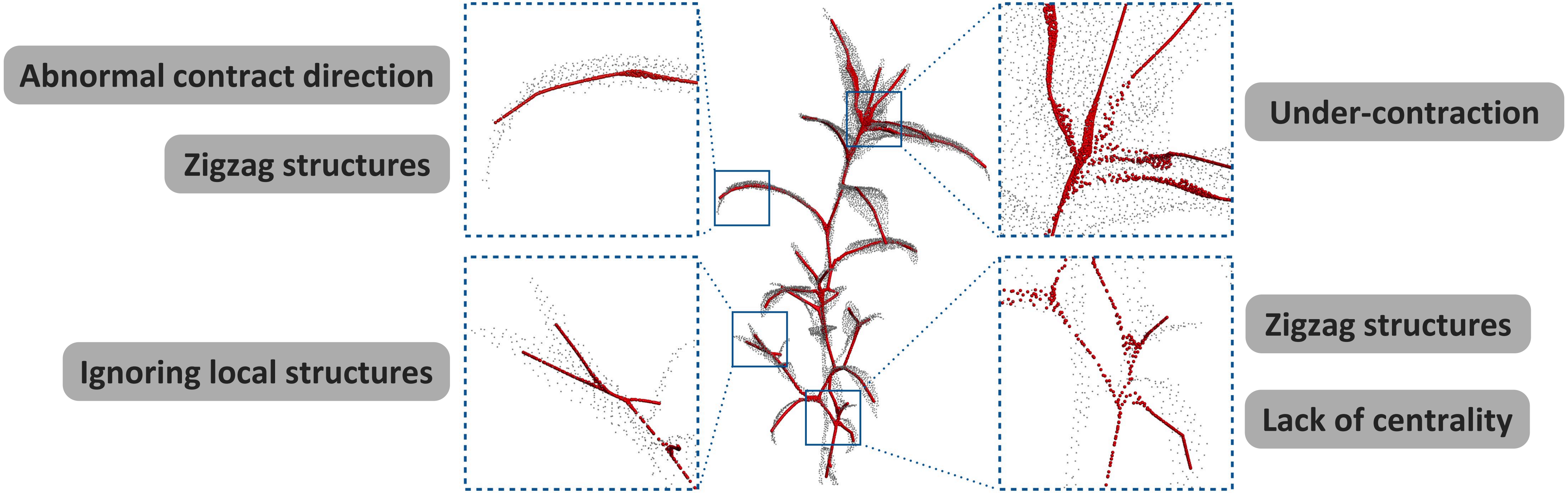

Methodology - Point Cloud Contraction

➢ Constraint Laplacian Operator

- Abnormal contract direction; Zigzag structures; Ignore local structures can be addressed.

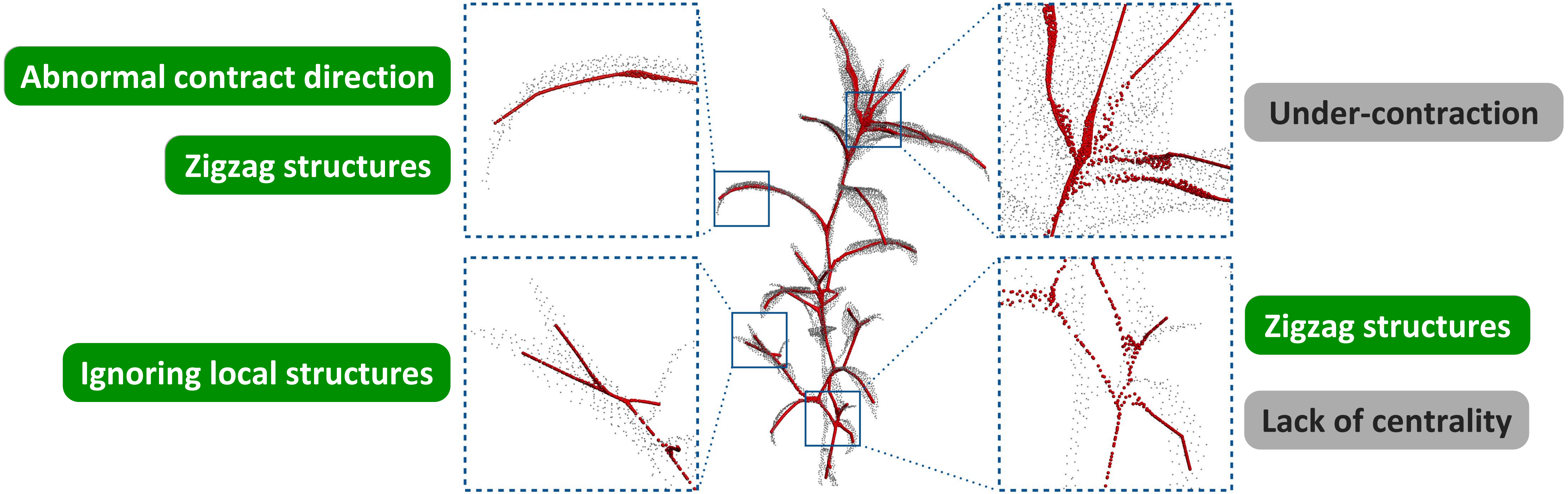

Methodology - Point Cloud Contraction

➢ Constraint Laplacian Operator

- Laplacian Operator

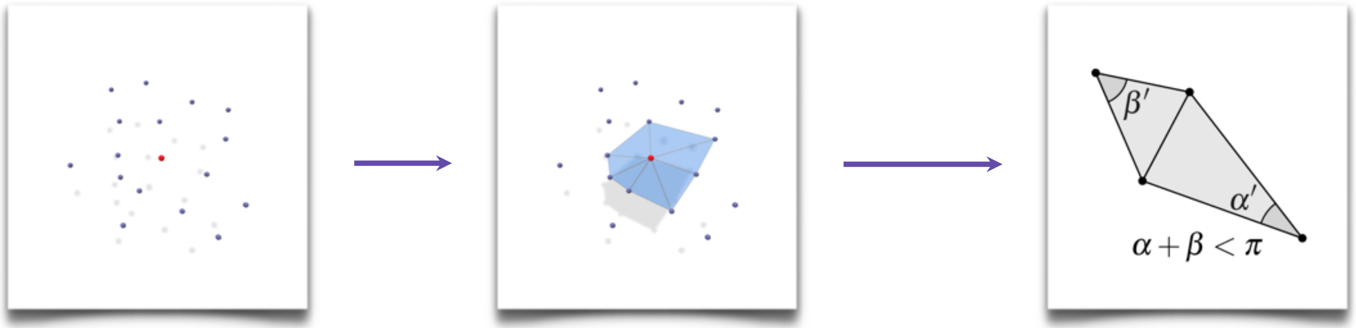

Local Delaunay condition:

$$\theta_k^{ij} + \theta_m ji \leq \pi$$

$$cot\theta_k^{ij} + cot\theta_M^{ji} \geq 0$$

Methodology - Point Cloud Contraction

➢ Constraint Laplacian Operator

- Laplacian Operator

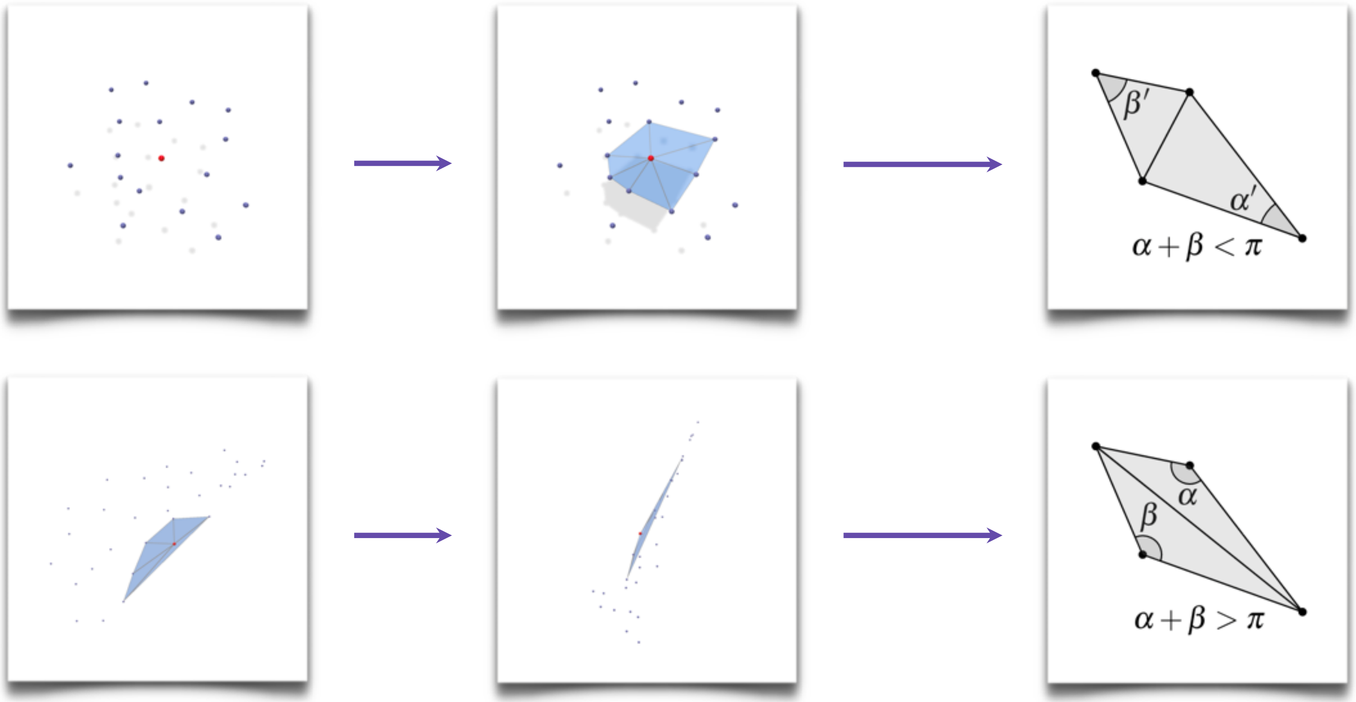

Local Delaunay condition:

$$\theta_k^{ij} + \theta_m ji \leq \pi$$

$$cot\theta_k^{ij} + cot\theta_M^{ji} \geq 0$$

Methodology - Point Cloud Contraction

➢ Constraint Laplacian Operator

- Tufted Laplacian Operator (**Sharp, N. and Crane, K., 2020.**)

Point cloud

k-nearest neighbors

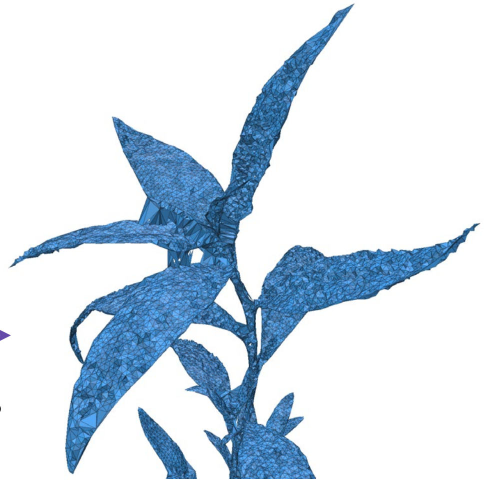

Union local triangles

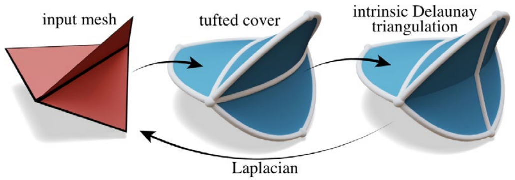

Tufted over

Tufted mesh

Tufted Laplacian Operator

Contraction directions

Methodology - Point Cloud Contraction

➢ Constraint Laplacian Operator

- Tufted Laplacian Operator
- Dynamic Neighbors Searching

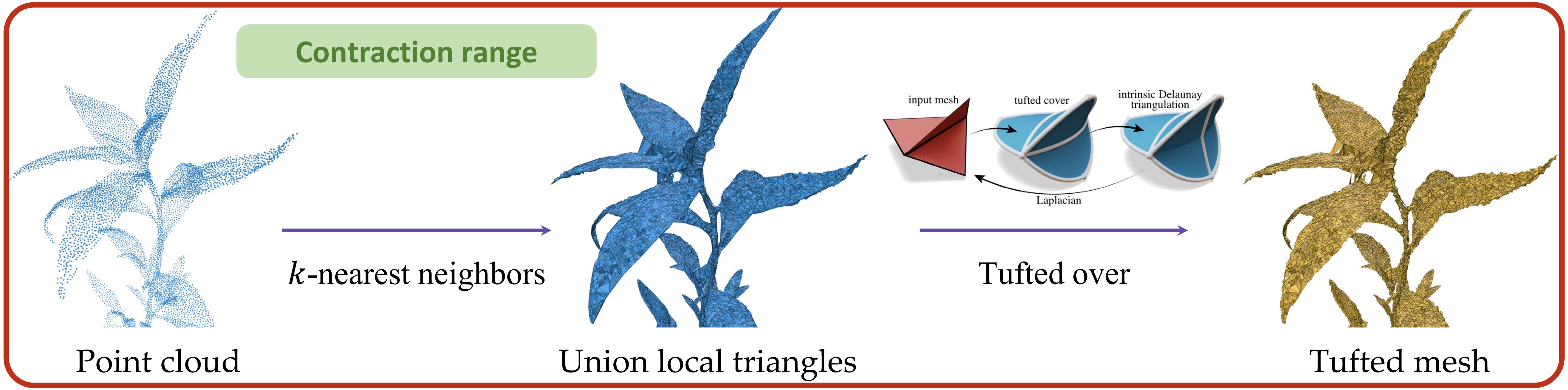

Methodology - Point Cloud Contraction

➢ Constraint Laplacian Operator

- Tufted Laplacian Operator
- Dynamic Neighbors Searching

Constrain the contraction range by manipulating k-nearest neighbors

$k = 30$

$k = 8$

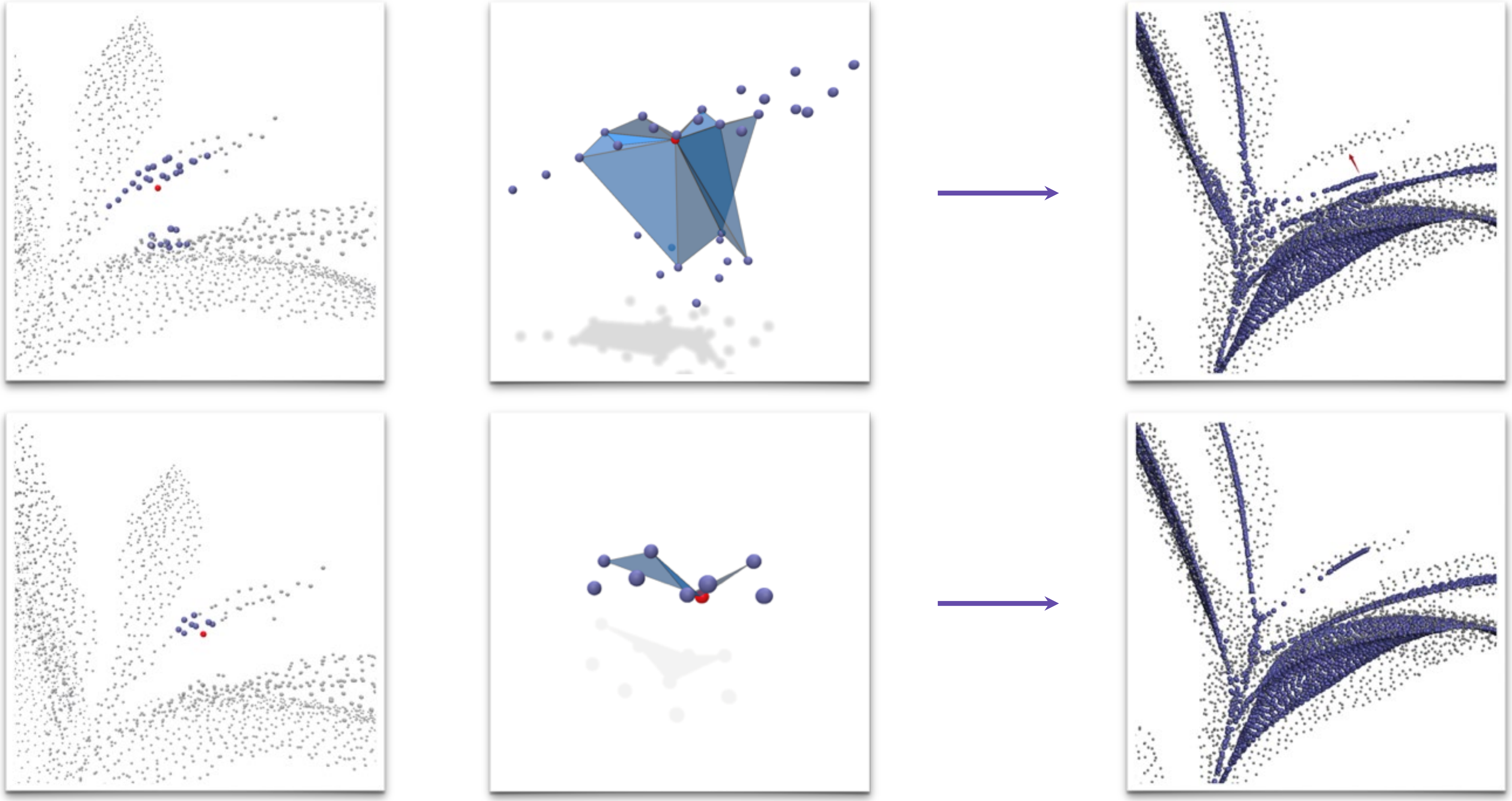

Methodology - Point Cloud Contraction

➢ Constraint Laplacian Operator

- Tufted Laplacian Operator
- Dynamic Neighbors Searching

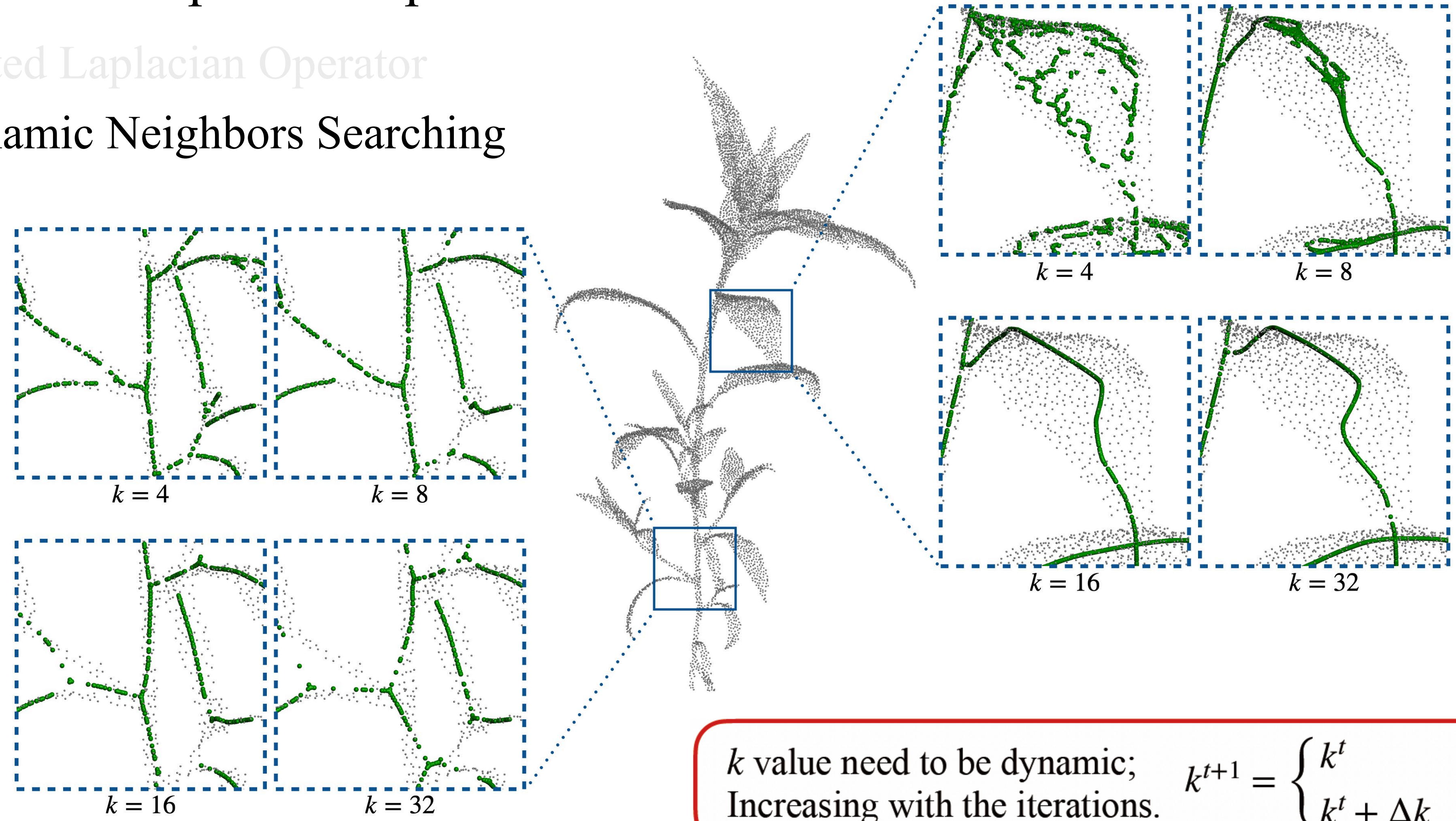

k value need to be dynamic;
Increasing with the iterations.

$$k^{t+1} = \begin{cases} k^t & k^t + \Delta k > k_{\max} \\ k^t + \Delta k & \text{otherwise} \end{cases}$$

Methodology - Point Cloud Contraction

➢ Constraint Laplacian Operator

- Tufted Laplacian Operator
- Dynamic Neighbors Searching
- Edge Collapse (Collapse long edges (≥ 3 · SD) among the Union local triangles)

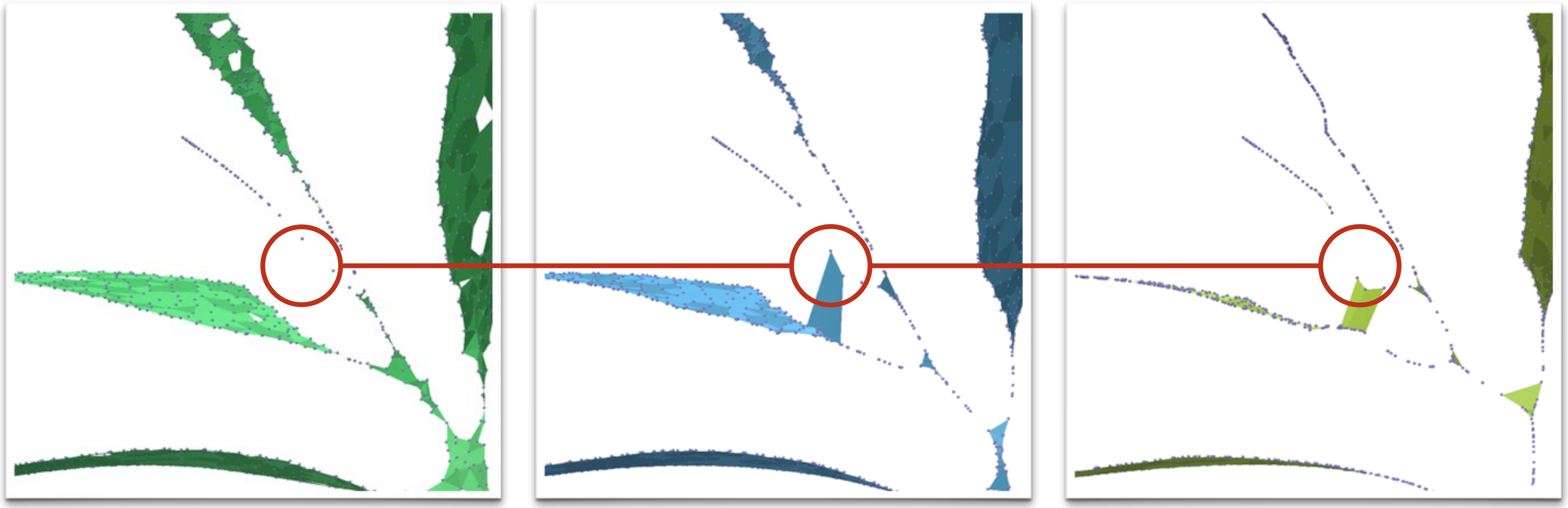

Iteration 1, $k = 8$ Iteration 2, $k = 12$ Iteration 3, $k = 16$

TUDelft

Methodology - Point Cloud Contraction

➢ Adaptive Contraction

- Under-contraction; Some refinements.

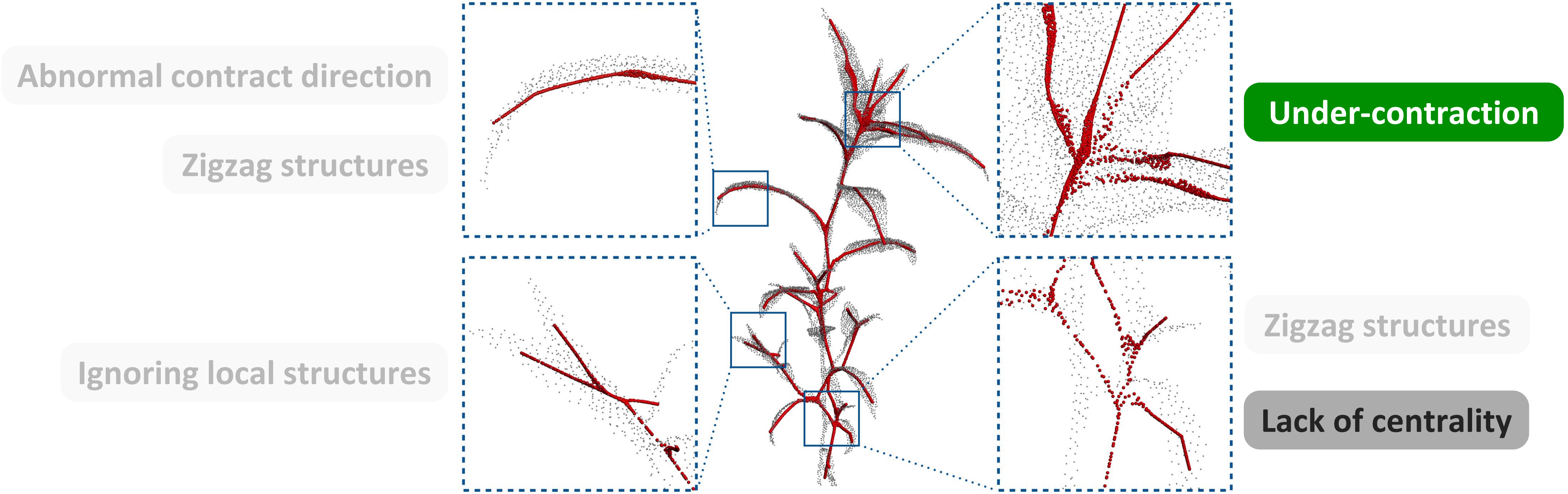

Methodology - Point Cloud Contraction

➢ Adaptive Contraction

- Directionality-based Weighting

$$\mathbf{cov}_i = \sum_{i' \in I \setminus \{i\}} \theta\left(\|p_i - p_{i'}\|\right)\left(p_i - p_{i'}\right)^{\top}\left(p_i - p_{i'}\right)$$

$$\theta(x) = e^{\frac{-x^2}{(h/2)^2}}$$

$$\boxed{\sigma_i = \frac{\lambda_i^2}{\lambda_i^0 + \lambda_i^1 + \lambda_i^2}, \quad \text{where } \lambda_i^0 \leq \lambda_i^1 \leq \lambda_i^2}$$

Huang et al., 2013; Wang et al., 2017.

Methodology - Point Cloud Contraction

➢ Adaptive Contraction

- Directionality-based Weighting

$$\mathbf{cov}_i = \sum_{i' \in I \setminus \{i\}} \theta\left(\|p_i - p_{i'}\|\right) \left(p_i - p_{i'}\right)^{\top} \left(p_i - p_{i'}\right)$$

$$\theta(x) = e^{\frac{-x^2}{(h/2)^2}}$$

$$\boxed{\sigma_i = \frac{\lambda_i^2}{\lambda_i^0 + \lambda_i^1 + \lambda_i^2}, \quad \text{where } \lambda_i^0 \leq \lambda_i^1 \leq \lambda_i^2}$$

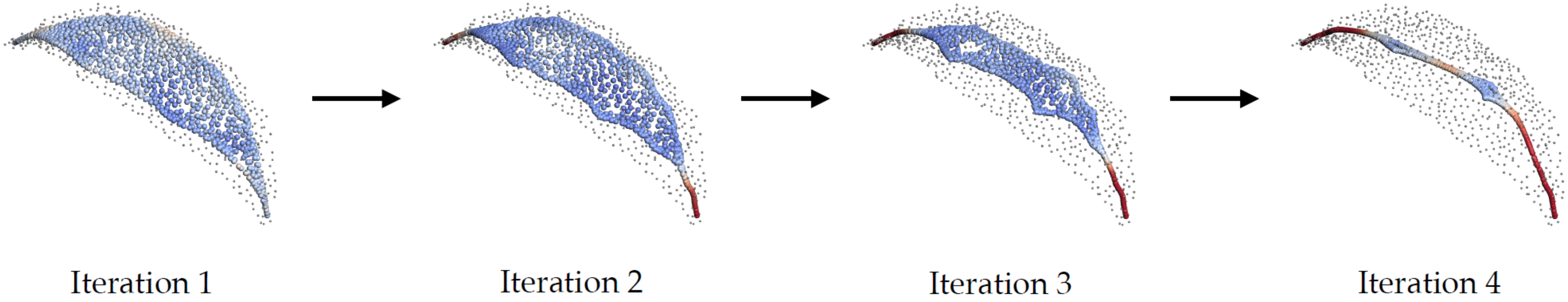

Huang et al., 2013; Wang et al., 2017.

Methodology - Point Cloud Contraction

➢ Adaptive Contraction

- Directionality-based Weighting

$$\mathbf{cov}_i = \sum_{i' \in I \setminus \{i\}} \theta\left(\|p_i - p_{i'}\|\right)\left(p_i - p_{i'}\right)^{\top}\left(p_i - p_{i'}\right)$$

$$\theta(x) = e^{\frac{-x^2}{(h/2)^2}}$$

$$\boxed{\sigma_i = \frac{\lambda_i^2}{\lambda_i^0 + \lambda_i^1 + \lambda_i^2}, \quad \text{where } \lambda_i^0 \le \lambda_i^1 \le \lambda_i^2}$$

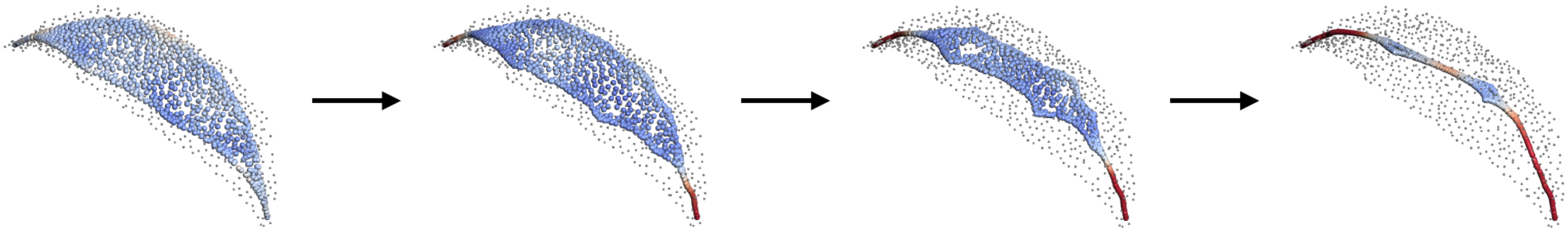

Iteration 1 Iteration 2 Iteration 3 Iteration 4

$$\mathbf{W}_{L,i}^{t+1} = \begin{cases} 0 & \text{smooth\_}\sigma_i^t \ge \epsilon \\ \mathbf{W}_{L,i}^t & \epsilon > \text{smooth\_}\sigma_i^t \ge \epsilon - 0.1 \\ s_L \mathbf{W}_{L,i}^t & \text{otherwise} \end{cases} \quad \mathbf{W}_{H,i}^{t+1} = \begin{cases} \phi & \text{smooth\_}\sigma_i^t \ge \epsilon \\ \mathbf{W}_{H,i}^t & \text{otherwise} \end{cases}$$

Huang et al., 2013; Wang et al., 2017.

Methodology - Point Cloud Contraction

➢ Adaptive Contraction

- Directionality-based Weighting
- Distance Constraint

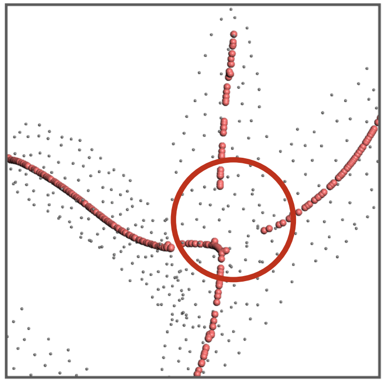

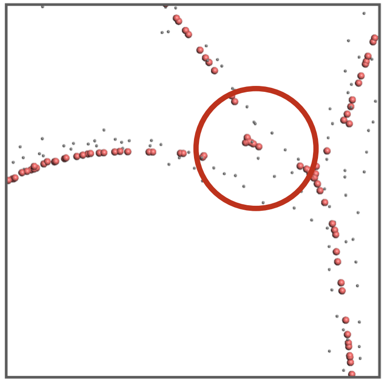

Weng et al., 2006.

Methodology - Point Cloud Contraction

➢ Adaptive Contraction

- Directionality-based Weighting
- Distance Constraint

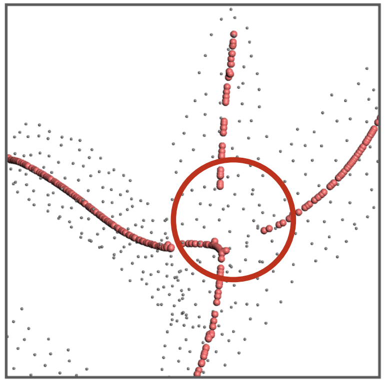

Spring only with attraction force

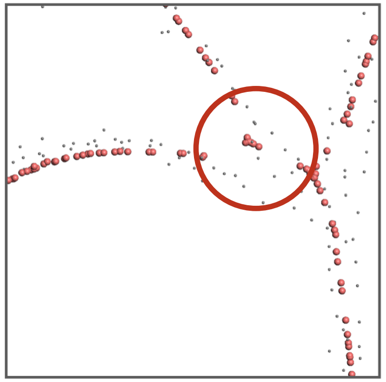

$$\sum_{(i,j)\in \mathrm{Edge}_{\mathcal{T}}} \left\| (p_i - p_j) - e(p_i, p_j) \right\|^2$$

$$e(p_i, p_j) = \begin{cases} (p_i - p_j) & \left\| p_i - p_j \right\|^2 \le d_{\max} \\ \dfrac{d_{\max}}{\left\| p_i - p_j \right\|^2}(p_i - p_j) & \left\| p_i - p_j \right\|^2 > d_{\max} \end{cases}$$

Weng et al., 2006.

Methodology - Point Cloud Contraction

➢ Adaptive Contraction

$$\begin{bmatrix} \mathbf{W}_L L \\ \mathbf{W}_H \end{bmatrix} \mathbf{P}^{t+1} = \begin{bmatrix} 0 \\ \mathbf{W}_H \mathbf{P}^t \end{bmatrix} \Longrightarrow \begin{bmatrix} \mathbf{W}_L L \\ \mathbf{W}_H \\ \mathbf{W}_D \mathbf{H}^t \end{bmatrix} \mathbf{P}^{t+1} = \begin{bmatrix} 0 \\ \mathbf{W}_H \mathbf{P}^t \\ \mathbf{W}_D e(\mathbf{P}^t) \end{bmatrix}$$

- Directionality-based Weighting
- Distance Constraint

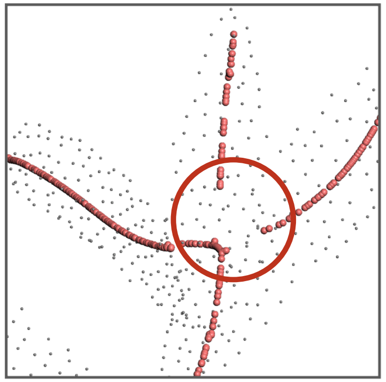

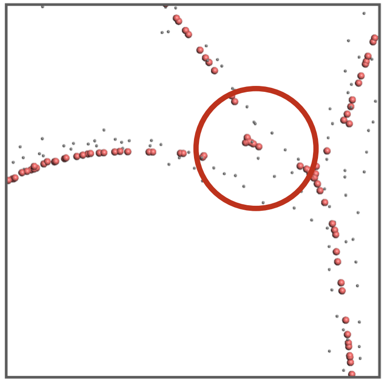

Spring only with attraction force

$$\sum_{(i,j)\in \mathrm{Edge}_{\mathcal{T}}} \left\| (p_i - p_j) - e(p_i, p_j) \right\|^2$$

$$e(p_i, p_j) = \begin{cases} (p_i - p_j) & \left\| p_i - p_j \right\|^2 \le d_{\max} \\ \dfrac{d_{\max}}{\left\| p_i - p_j \right\|^2}(p_i - p_j) & \left\| p_i - p_j \right\|^2 > d_{\max} \end{cases}$$

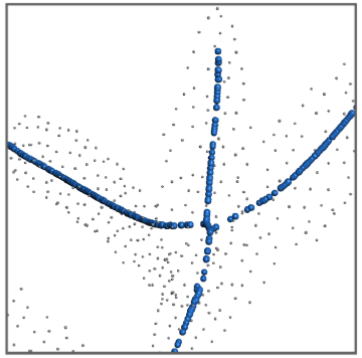

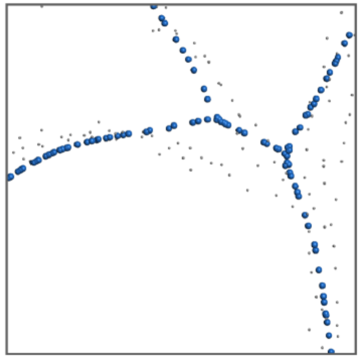

Weng et al., 2006.

Methodology - Point Cloud Contraction

➢ Tip points preservation

- Offset at leaf tip region

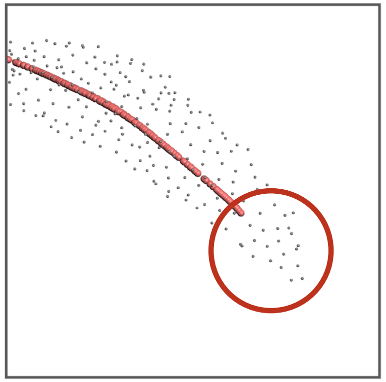

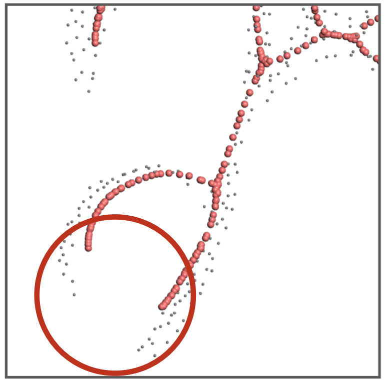

Crane et al., 2017.

Methodology - Point Cloud Contraction

➢ Tip points preservation

- Offset at leaf tip region

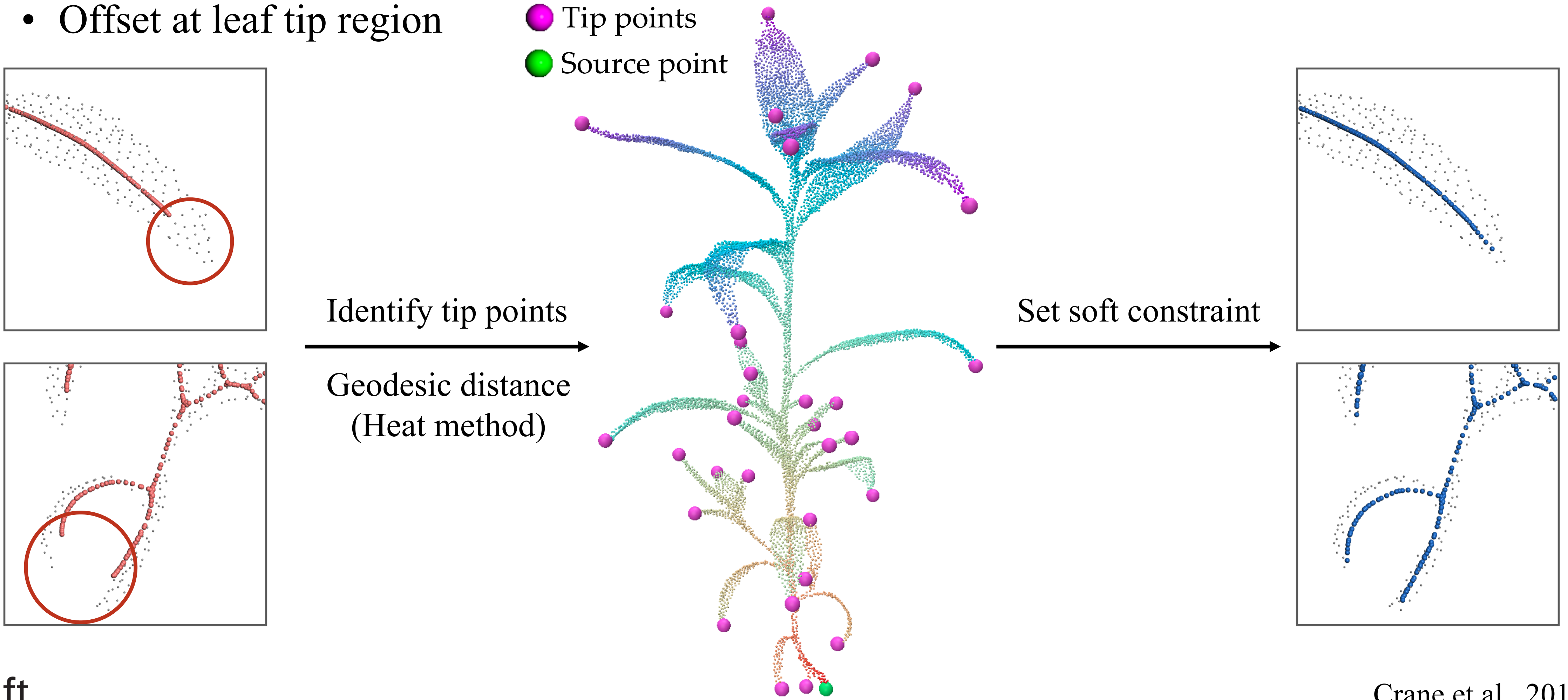

Crane et al., 2017.

Methodology - Skeleton Graph Generation

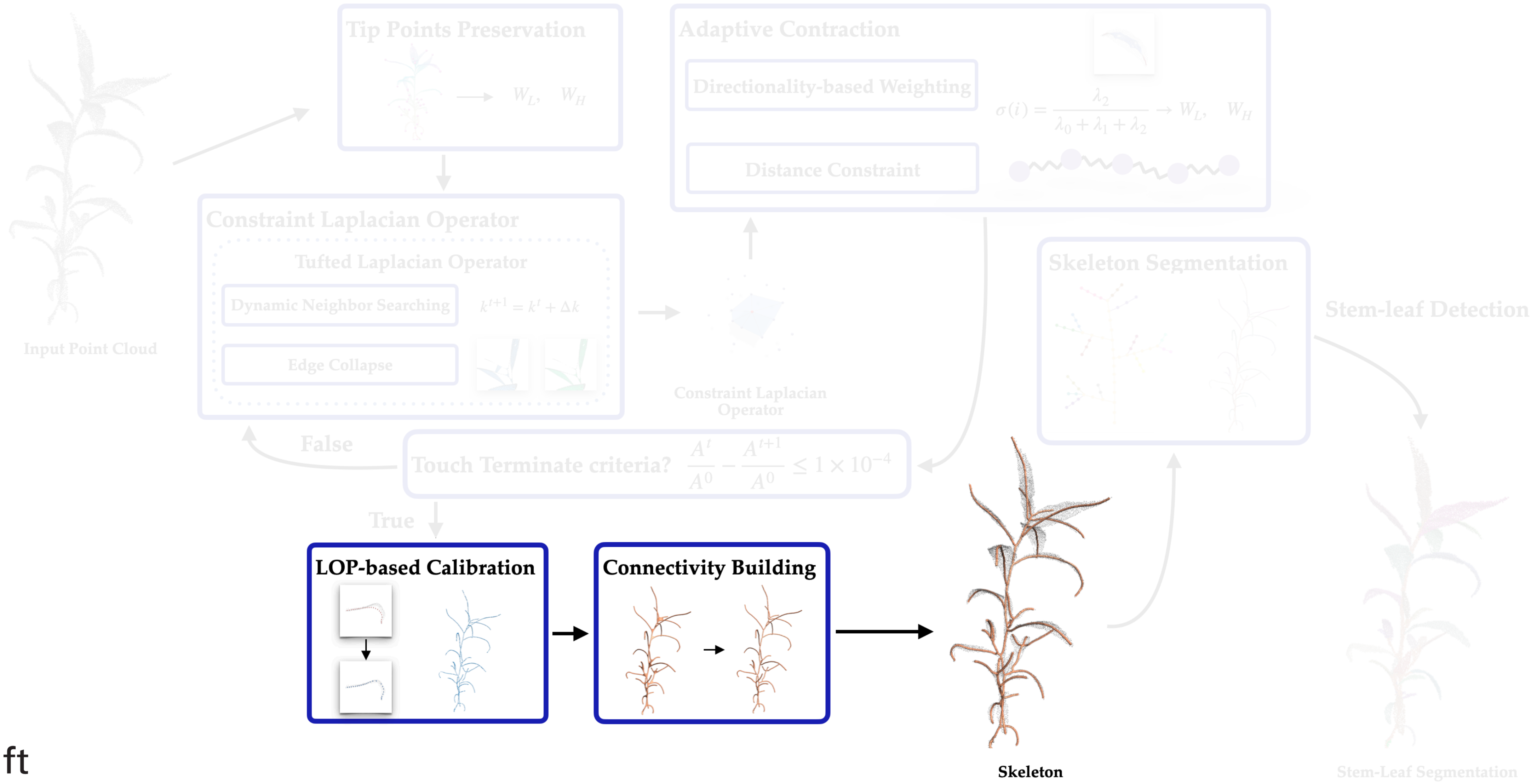

TUDelft

Methodology - Skeleton Graph Generation

➢ LOP-based Calibration

- Lack of centrality.

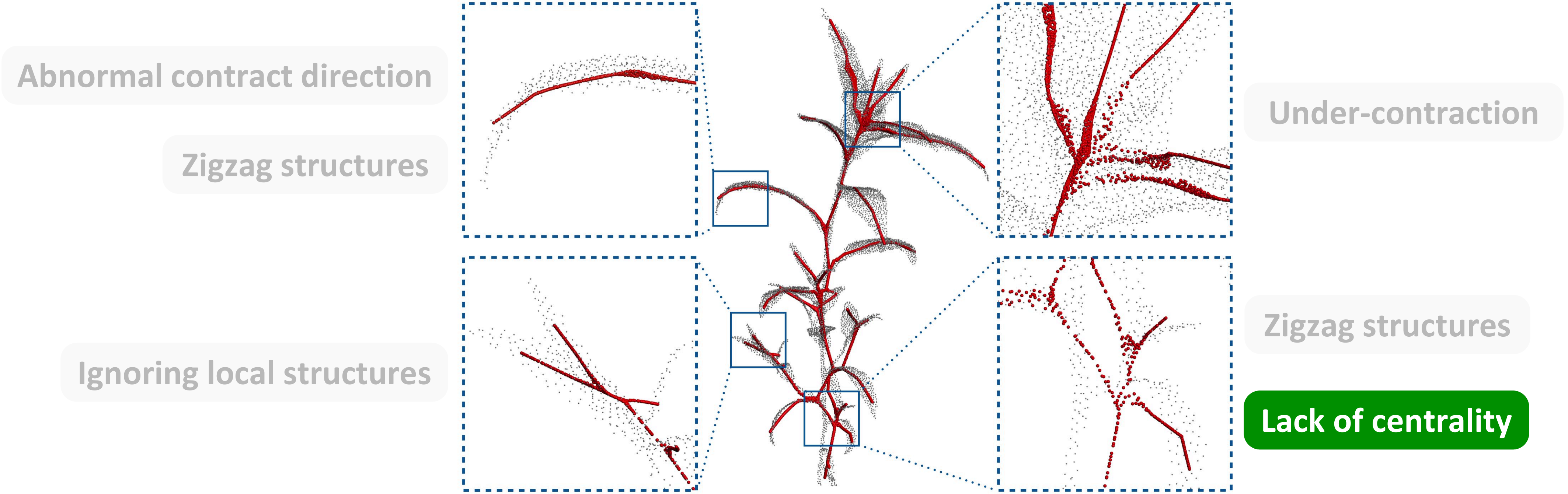

Methodology - Skeleton Graph Generation

➢ LOP-based Calibration

- Farthest point downsampling

Methodology - Skeleton Graph Generation

➢ LOP-based Calibration

- Farthest point downsampling $\Longrightarrow$ Modified LOP (Locally Optimal Projection) operator

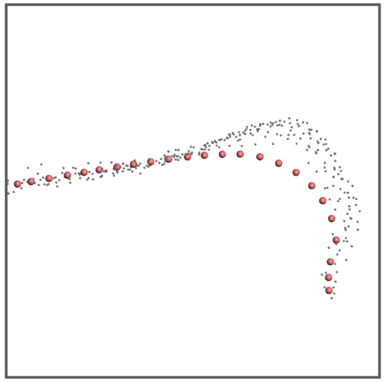

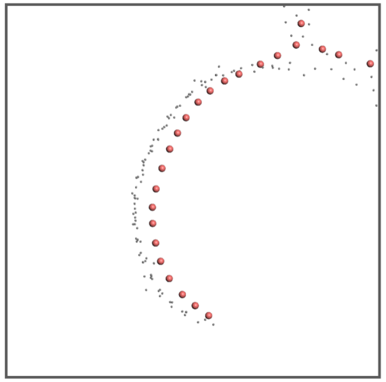

$$x_i^{(t+1)} = \boxed{\sum_{j\in N} q_j \frac{\alpha_j^i}{\sum_{j\in N}\alpha_j^i}} + \mu \sum_{j\in N\backslash\{i\}} \left(x_i^{(t)} - x_j^{(t)}\right) \frac{\beta_j^i}{\sum_{j\in N\backslash\{i\}}\beta_j^i}$$

$\downarrow$

Only reserved L_1 median term

$$x_i^{New} = \frac{\sum_{j\in K} p_j \alpha_{ij}}{\sum_{j\in K}\alpha_{ij}}, where \alpha_{ij} = \frac{\theta(\| p_i^t - q_j \|)}{\| x_i - q_j \|}$$

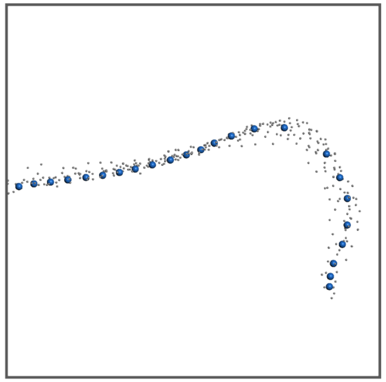

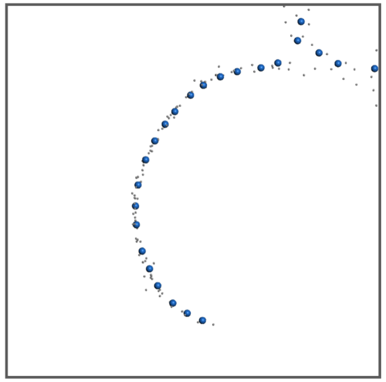

Lipman et al., 2007; Huang et al., 2013; Li and Wang, 2018.

Methodology - Skeleton Graph Generation

- ➢ Connectivity building
  - Build initial graph
  - Compute MST (Minimum Spanning Tree)
  - Pruning noisy branches

Initial Graph

Computed MST

Methodology - Stem-Leaf Segmentation

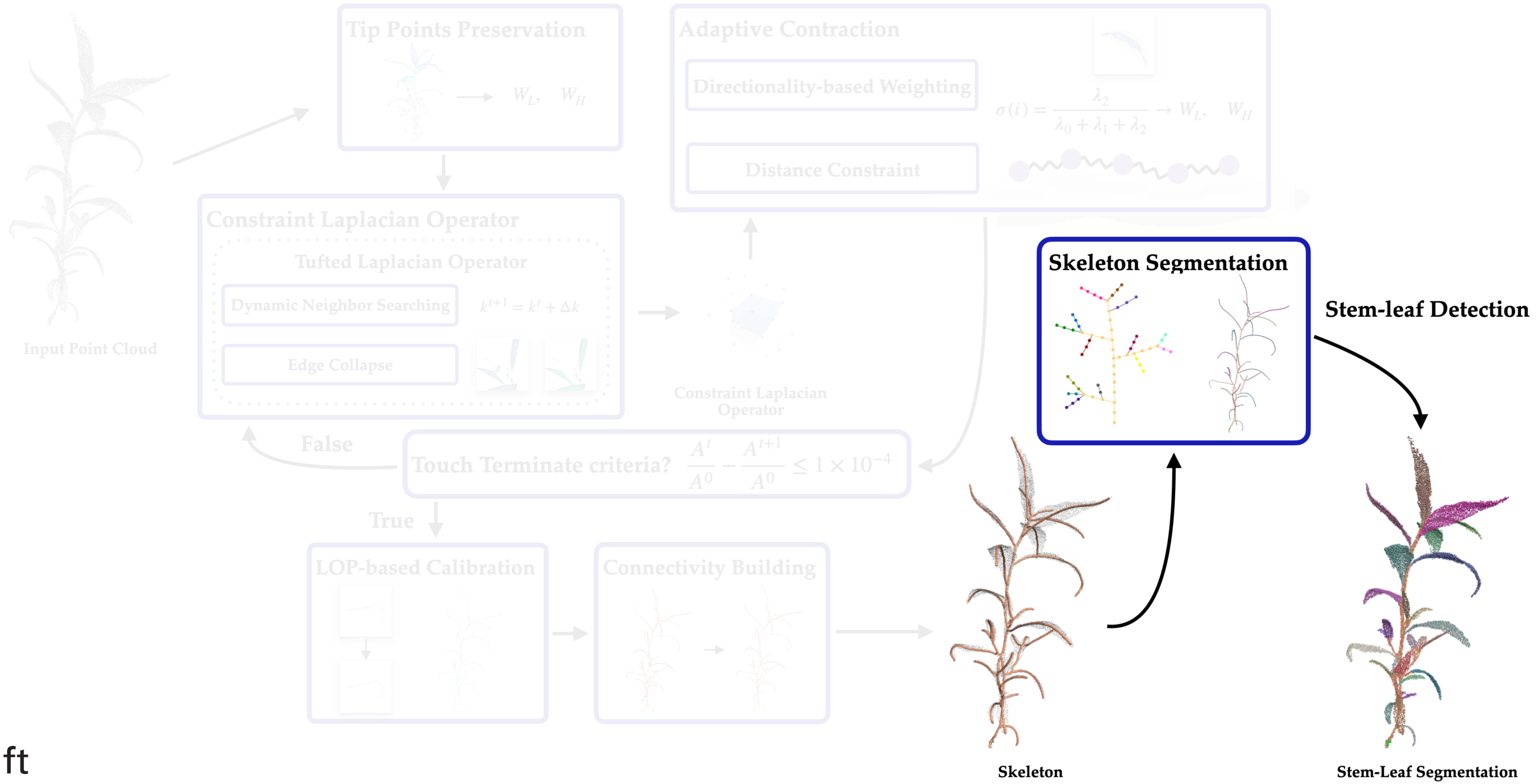

Methodology - Stem-Leaf Segmentation

➢ Skeleton Segmentation

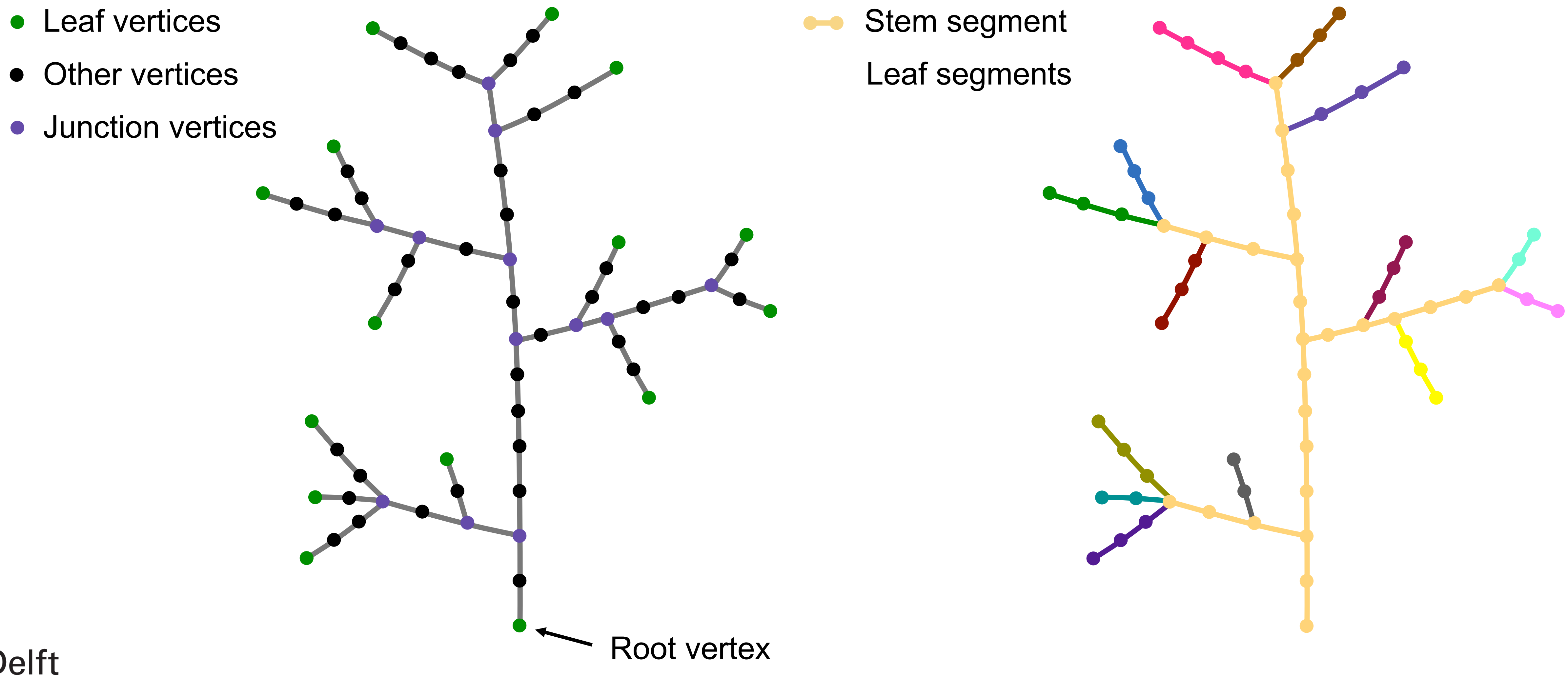

Methodology - Stem-Leaf Segmentation

➢ Stem-leaf detection

- Utilizing the nearest neighbor projection strategy

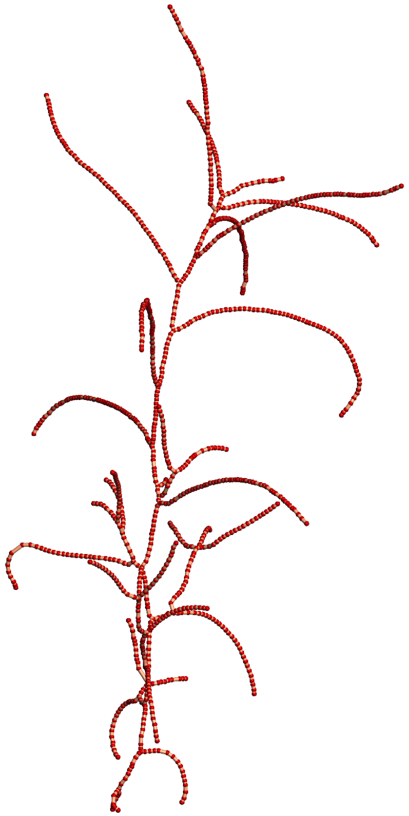

Skeleton

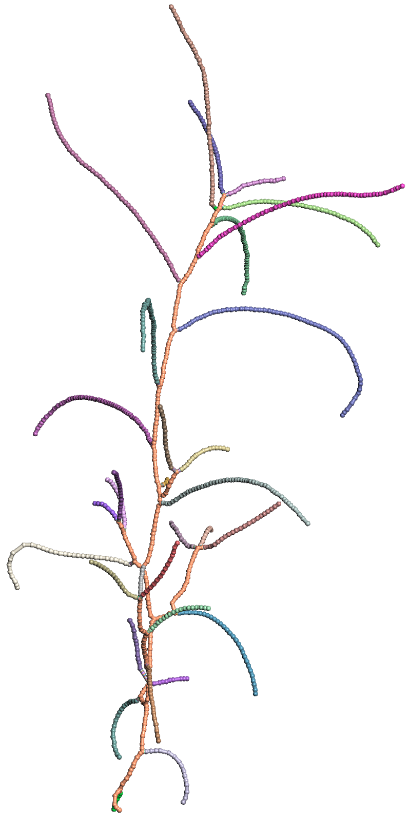

Skeleton Segmentation

Stem-Leaf Segmentation

Methodology - Photogrammetric Dataset

➢ 56 leafy plants

- with several later stems and multiple leaves;
- with various shapes (existing cylindric and planar shapes);
- with tiny structures.

Polygonum plants in wild environments

Polygonum lapathifolium

Methodology - Photogrammetric Dataset

➢ Image data acquisition (>100 for each plant)

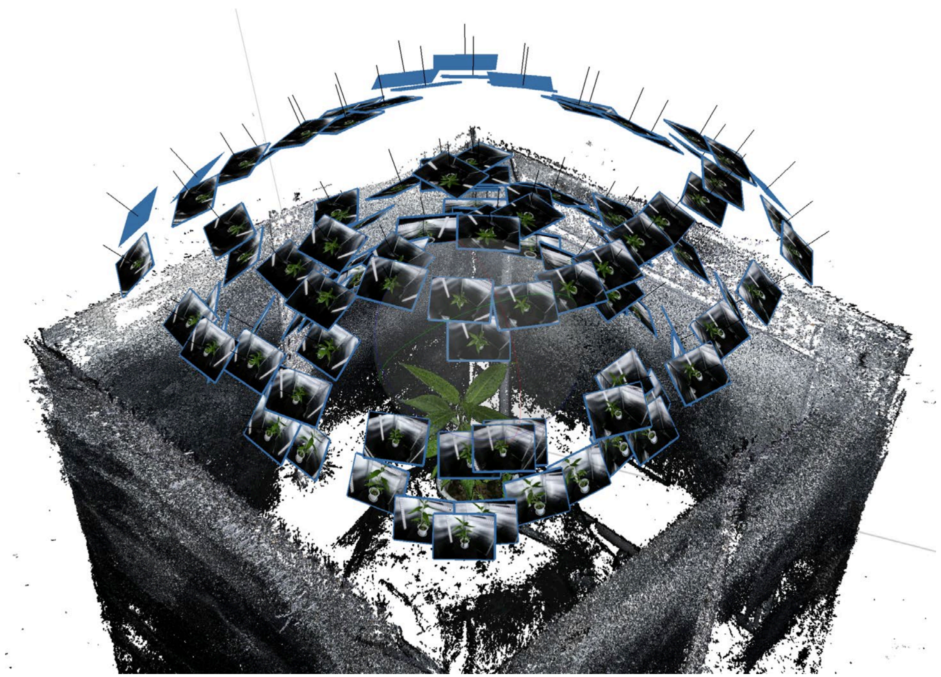

Captured multi-view image sequence

➢ Final point cloud data

Results & Discussion

Results

➢ Skeleton extraction results (default parameter settings)

Left: Discrete skeleton points; Right: Skeleton

Results

➢ Semantic segmentation results (default parameter settings)

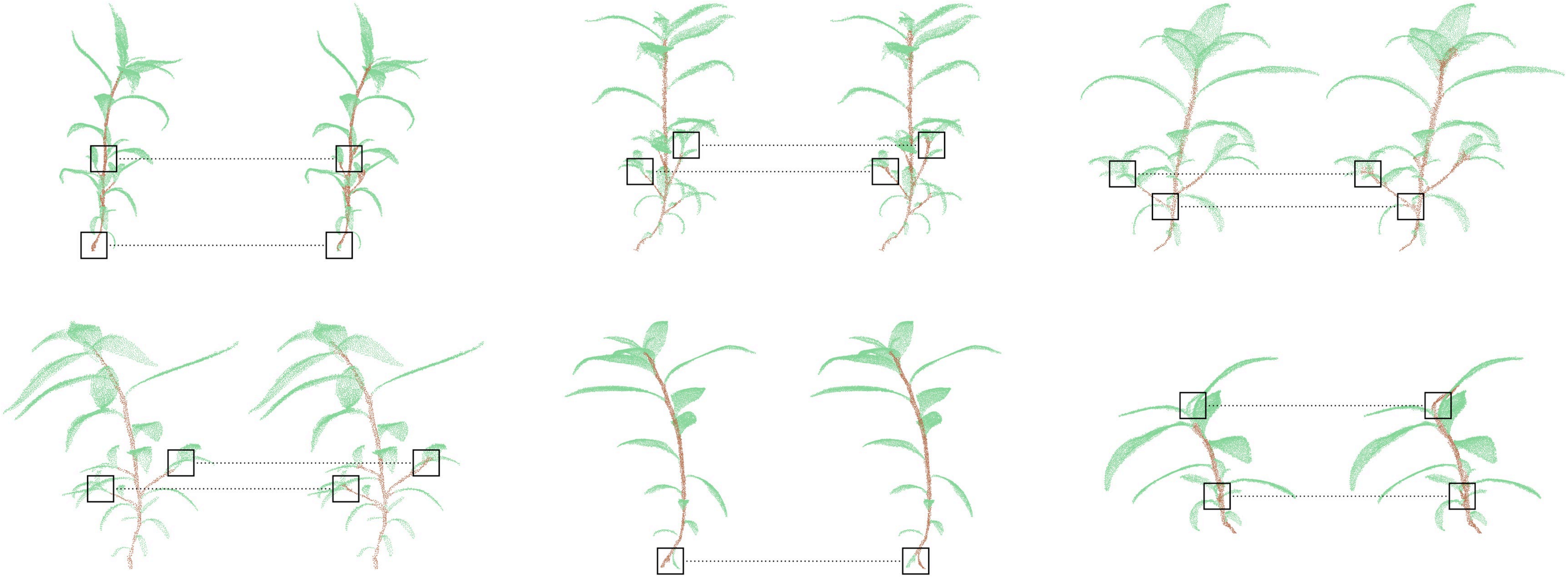

Left: Ground truth; Right: Predicted results

Results

➢ Instance segmentation results (default parameter settings)

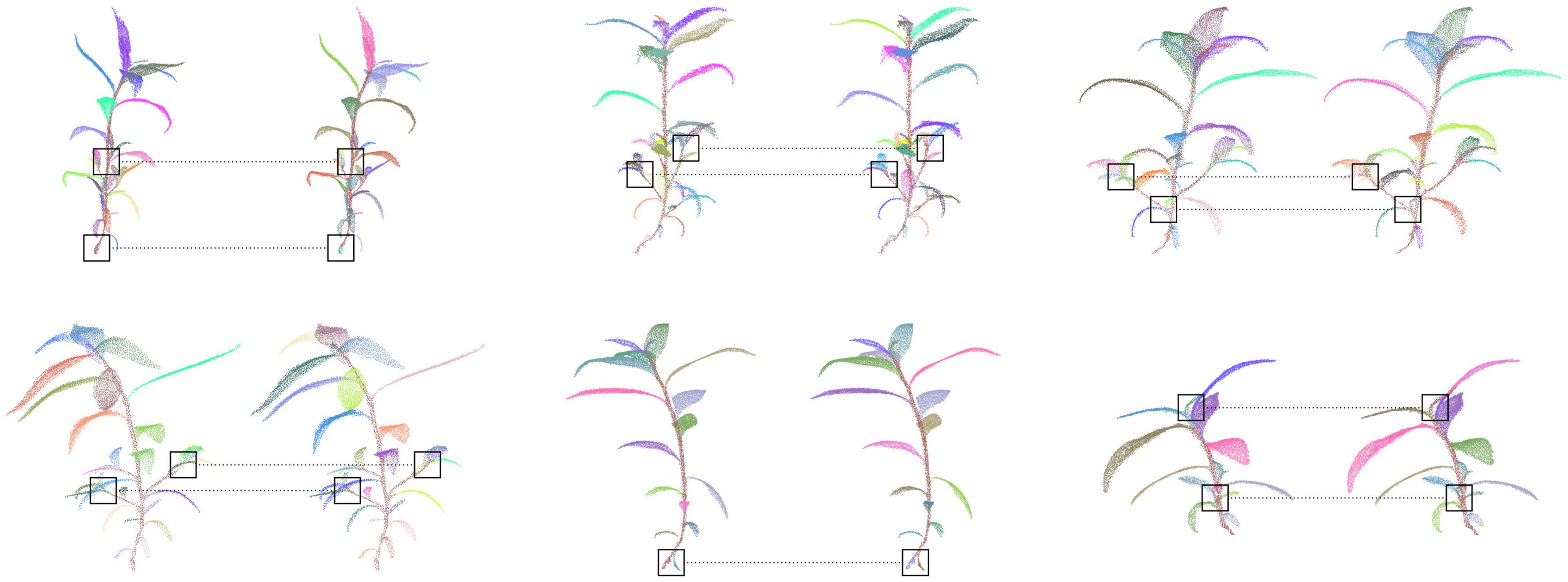

Left: Ground truth; Right: Predicted results

Results

➢ Quantitative metrics for segmentation results

Table 1. The quantitative metrics of stem-leaf semantic segmentation results

Metric	Stem	Leaf	Mean
$\mathrm{Prec}_{\mathrm{sem}}$ (%)	68.83	99.77	84.30
$\mathrm{Rec}_{\mathrm{sem}}$ (%)	97.40	96.25	96.83
F_1-score (%)	80.66	97.98	89.32
IoU (%)	67.59	96.04	81.81

$> 95\%$

Table 2. The quantitative metrics of leaf instance segmentation results

	$\mathrm{Prec}_{\mathrm{ins}}$ (%)	$\mathrm{Rec}_{\mathrm{ins}}$ (%)	mCov (%)	mWCov (%)
Leaf	96.13	93.13	85.00	94.66

$\geq 85\%$

Discussion

➢ Skeleton quality comparison

- Other skeletonization algorithms
  - **LBC (Cao et al., 2010)**
  - **L_1-medial (Huang et al., 2013)**
  - **AdTree (Du et al., 2019)**
  - **WoodSKE (Wu et al., 2021)**

TU Delft

Cao et al., 2010; Huang et al., 2013; Du et al., 2019; Wu et al., 2021.

Discussion

➢ Skeleton quality comparison

- Other skeletonization algorithms
  - **LBC (Cao et al., 2010)**
  - **L_1-medial (Huang et al., 2013)**
  - **AdTree (Du et al., 2019)**
  - **WoodSKE (Wu et al., 2021)**

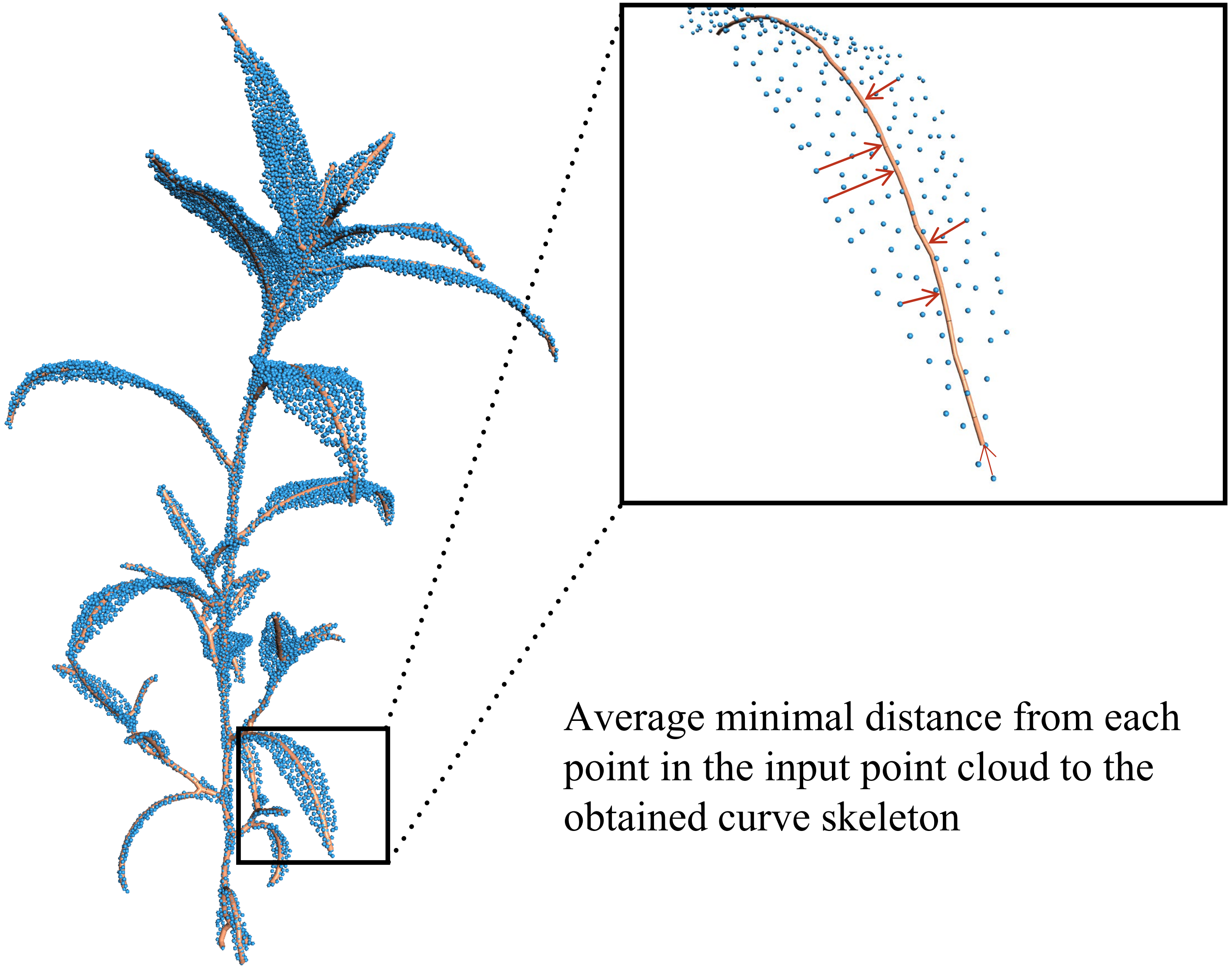

Average minimal distance from each point in the input point cloud to the obtained curve skeleton

Cao et al., 2010; Huang et al., 2013; Du et al., 2019; Wu et al., 2021.

Discussion

➢ Skeleton quality comparison (Plant-A)

Ours LBC L_1-medial AdTree WoodSKE

Table 3a. The quantitative metric of skeleton extraction results (a lower is better)

Ours	LBC	L_1-medial	AdTree	WoodSKE
0.021065	0.026008	0.032905	0.006505	0.037584

Discussion

➢ Skeleton quality comparison (Plant-A)

Ours LBC L_1-medial AdTree WoodSKE

Table 3a. The quantitative metric of skeleton extraction results (a lower is better)

Ours	LBC	L_1-medial	AdTree	WoodSKE
0.021065	0.026008	0.032905	0.006505	0.037584

Discussion

➢ Skeleton quality comparison (Plant-A)

Table 3a. The quantitative metric of skeleton extraction results (a lower is better)

Ours	LBC	L_1-medial	AdTree	WoodSKE
0.021065	0.026008	0.032905	~~0.006505~~	0.037584

Discussion

➢ Skeleton quality comparison (Plant-B)

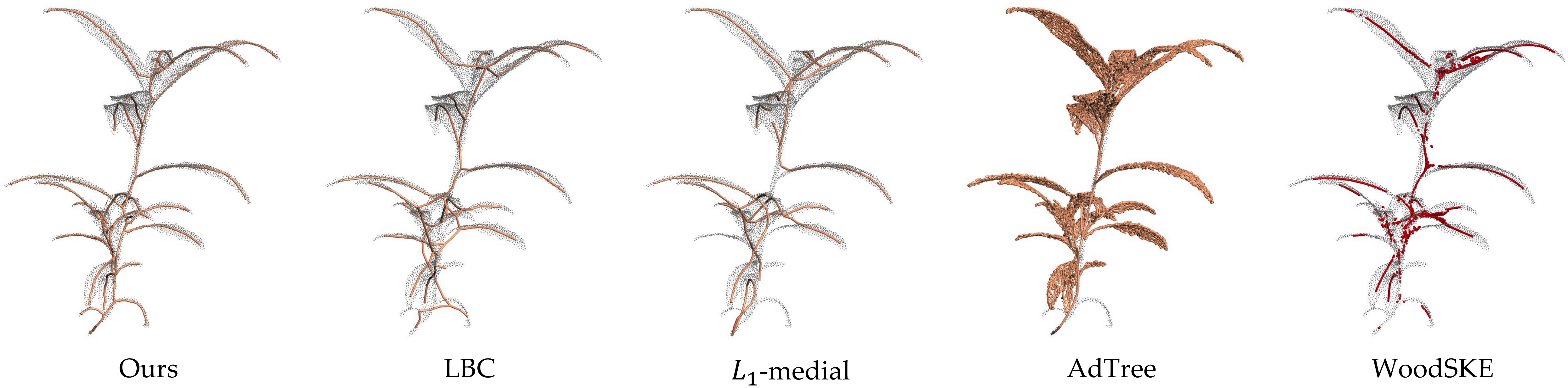

Table 3b. The quantitative metric of skeleton extraction results

Ours	LBC	L_1-medial	AdTree	WoodSKE
$\boxed{0.031357}$	0.037931	0.042576	~~0.007704~~	0.041590

Discussion

➢ Skeleton quality comparison (Plant-C)

Ours LBC L_1-medial AdTree WoodSKE

Table 3c. The quantitative metric of skeleton extraction results

Ours	LBC	L_1-medial	AdTree	WoodSKE
$\boxed{0.031330}$	0.035297	0.042870	~~0.009241~~	0.049664

Discussion

➢ Skeleton quality comparison (Plant-D)

Ours | LBC | L_1-medial | AdTree | WoodSKE

Table 3d. The quantitative metric of skeleton extraction results

Ours	LBC	L_1-medial	AdTree	WoodSKE
0.029281	0.031664	0.033632	~~0.008823~~	0.035311

Discussion

➢ Skeleton extraction on other plant species

- Four leafy plants (Pheno4D and PLANest-3D datasets)

Maize

Pepper

Ribes

Rose

Schunck et al., 2021; Mertoğlu et al., 2024.

Discussion

➢ Skeleton extraction on other plant species

- Four leafy plants
- Parameter settings
  - **Small structures**
  - **Point cloud density**

Dynamic Neighbors Searching ⟶

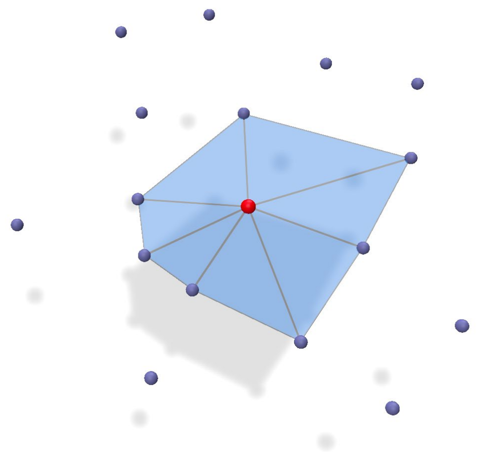

Constraint Laplacian Operator

KNN strategy

$$k^{t+1} = \begin{cases} k^t & k^t + \Delta k > k_{\max} \\ k^t + \Delta k & \text{otherwise} \end{cases}$$

Discussion

➢ Skeleton extraction on other plant species

- Four leafy plants
- Parameter settings
  - **Small structures**
  - **Point cloud density**

- More robust across diverse species;
- Relatively lower skeleton quality.

$\Uparrow$

KNN strategy

$$k^{t+1} = \begin{cases} k^t & k^t + \Delta k > k_{\max} \\ k^t + \Delta k & \text{otherwise} \end{cases}$$

$\Longrightarrow$

Ball query strategy

$$\boxed{rad^{t+1} = \begin{cases} rad^t & rad^t - \Delta rad < rad_{\min} \\ rad^t - \Delta rad & \text{otherwise} \end{cases}}$$

Discussion

➢ Skeleton extraction on other plant species

- Four leafy plants (Ball query strategy; Input #vertex=20480)

Maize
$rad^0 = 0.020 \cdot d_{bb}$

Pepper
$rad^0 = 0.020 \cdot d_{bb}$

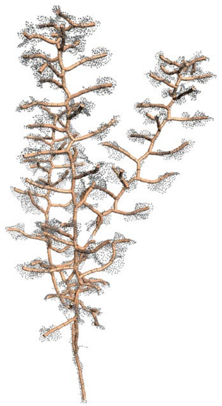

Ribes
$rad^0 = 0.020 \cdot d_{bb}$

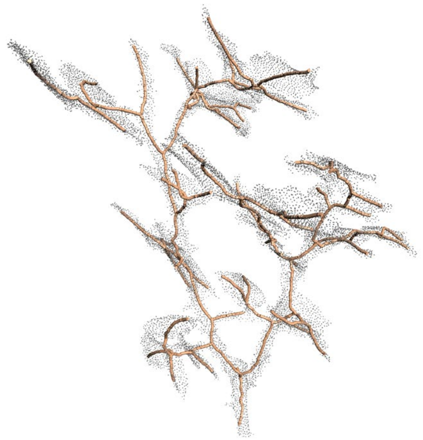

Rose
$rad^0 = 0.035 \cdot d_{bb}$

Discussion

➢ Skeleton extraction on other plant species

- Four different trees (TreeML-Data dataset; KNN strategy; Input #vertex=204800)

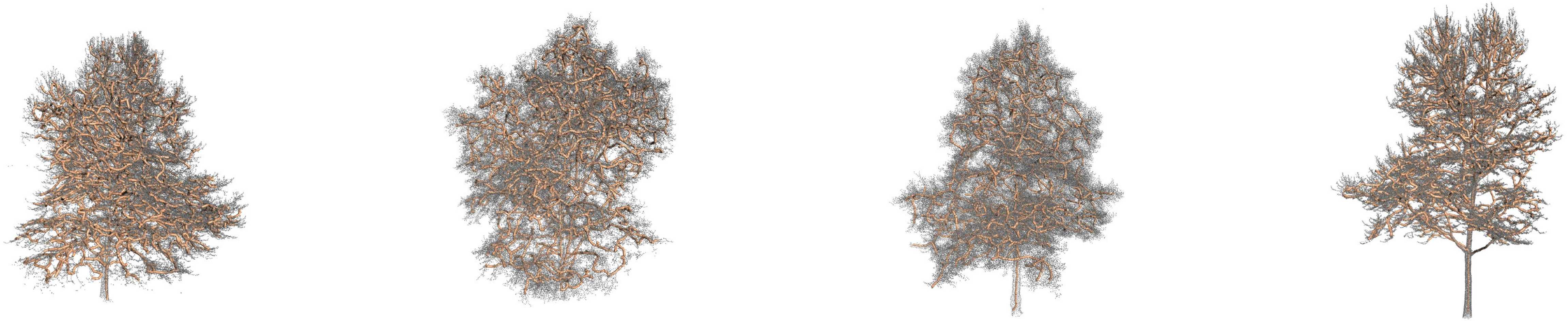

Tree A Tree B Tree C Tree D

Yazdi et al., 2024.

Discussion

➢ Skeleton extraction on other plant species

- Four different trees (TreeML-Data dataset; KNN strategy; Input #vertex=204800)

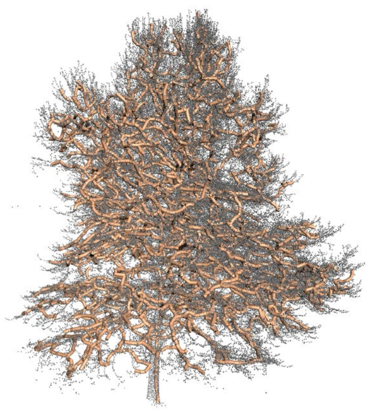

Tree A

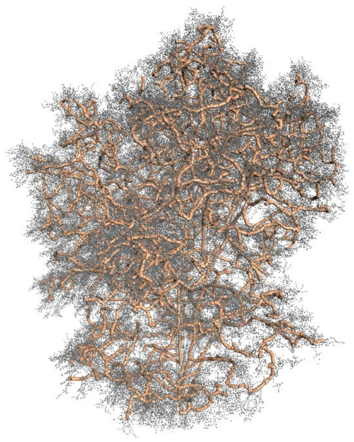

Tree B

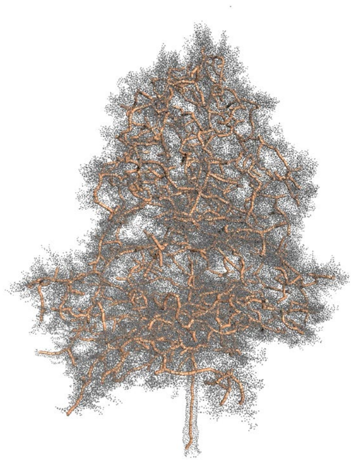

Tree C

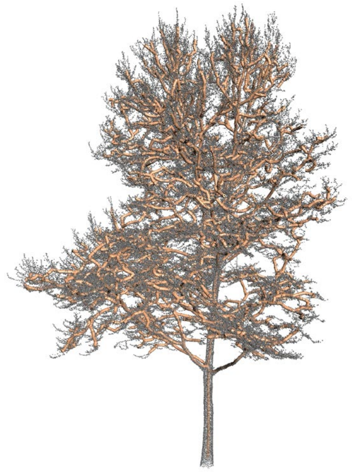

Tree D

TUDelft

Yazdi et al., 2024.

Discussion

➢ Computation complexity (default parameter settings)

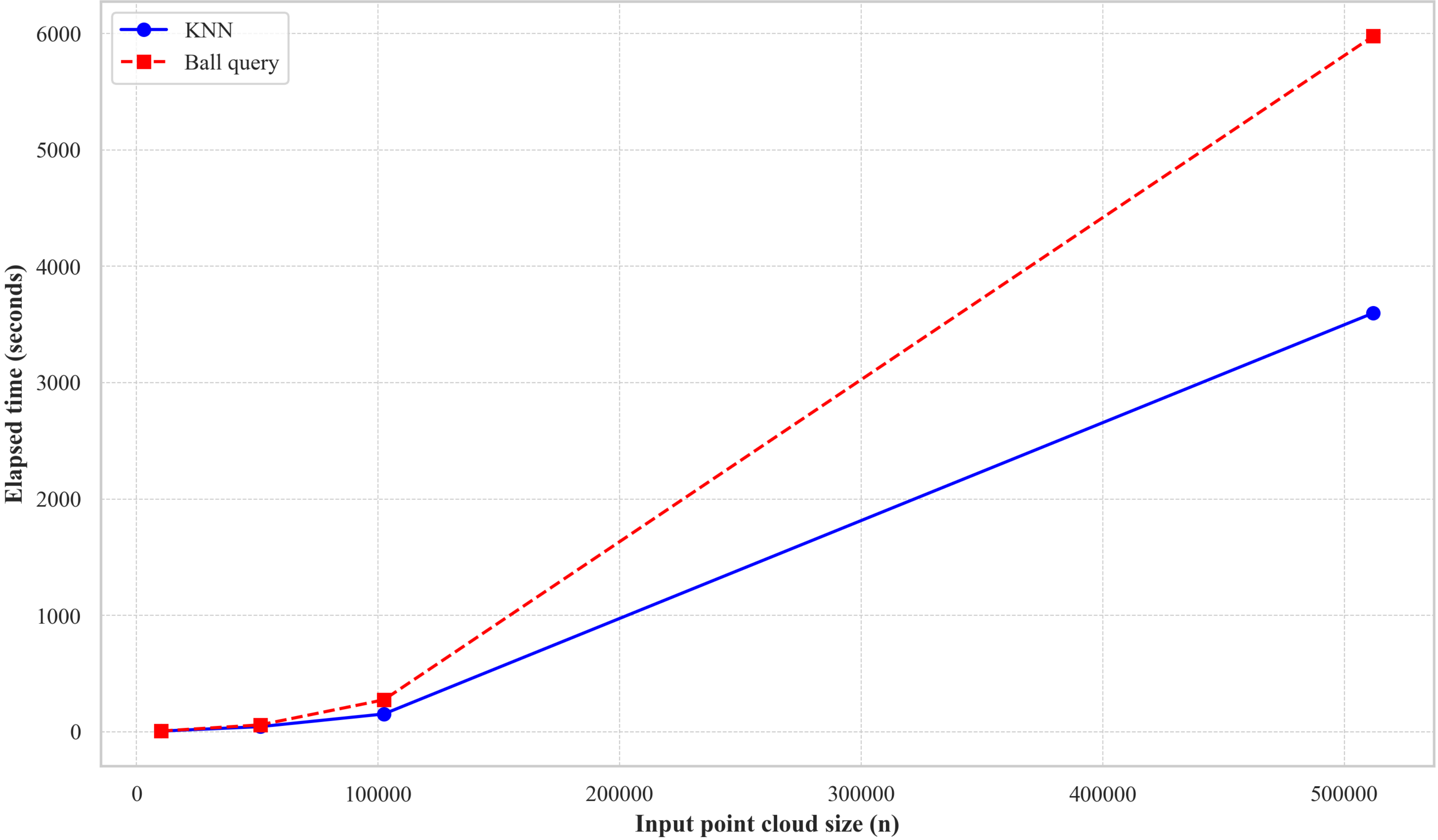

Discussion

➢ Computation complexity (default parameter settings)

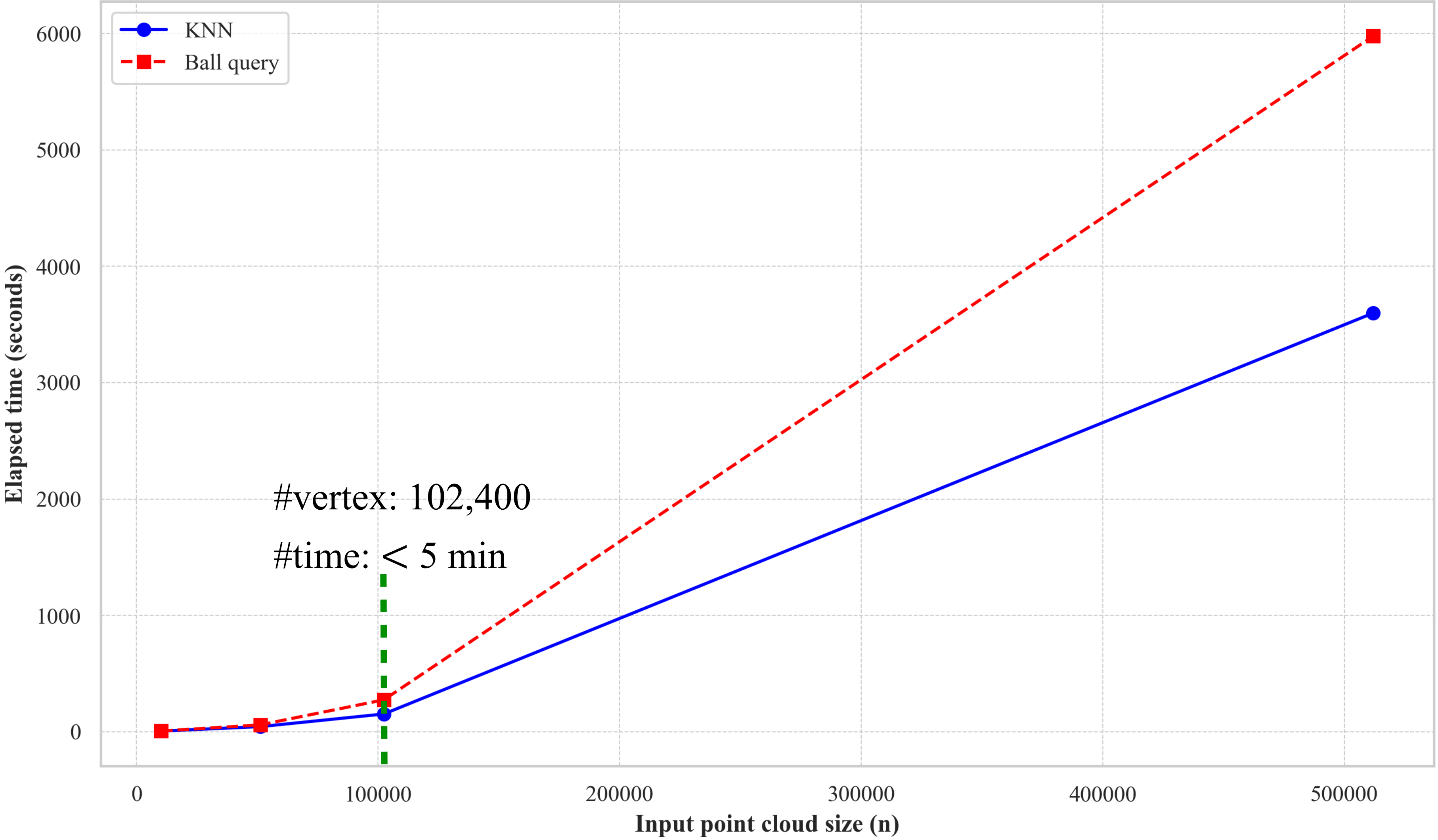

Limitations

➢ Data-driven, sensitive to the quality of point cloud;

➢ The approach to identify root vertex is not robust;

➢ Can only establish stem-leaf, two classes, segmentation.

Potential applications

➢ Organ segmentation

- Organ number count
- Volume measurements

➢ Leaf length

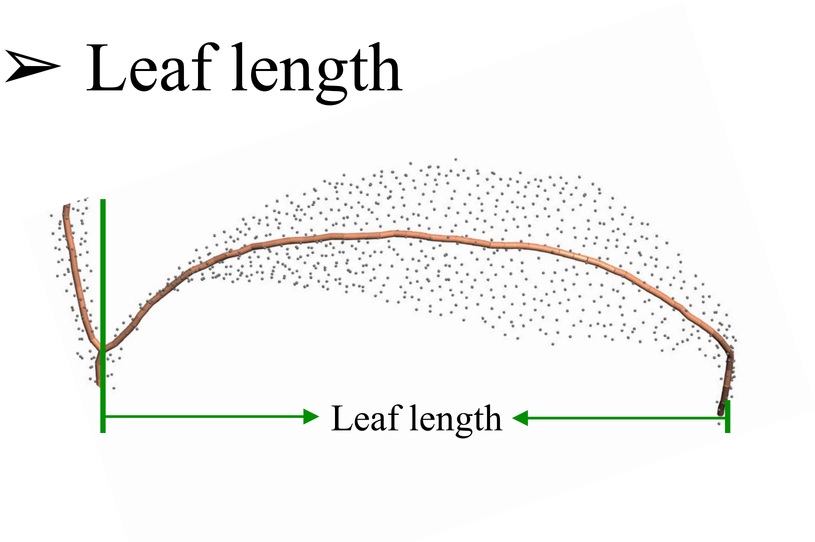

➢ Leaf angle

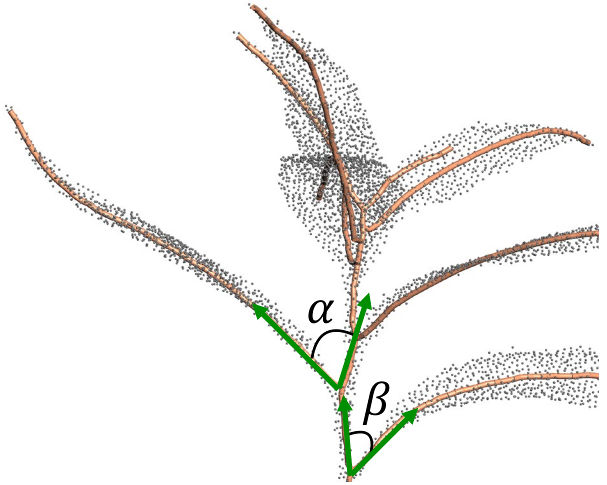

➢ Main stem length

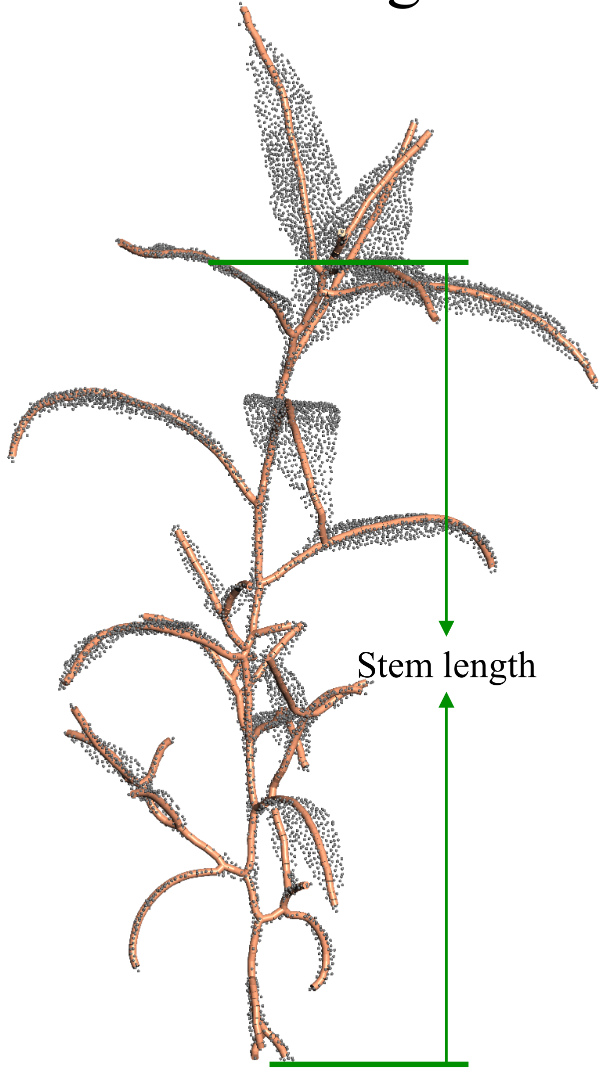

Conclusion & Future Work

Conclusion

- ➢ Can extract precise skeletons from leafy plants, which with complex later stems and multiple leaves, performing well on both leaves and stems, and then establish stem-leaf segmentation.

- ➢ Can robustly process various shapes and sizes of plants.

Image from www.clipstudio.net

Future Work

- A robust approach to identifying root vertex (e.g., user interaction);
- Impose biological prior knowledge to avoid potential incorrect branch connections;
- Regard the curve skeleton as a type of data argument, to boost the deep learning-based plant organ segmentation development.

Thanks for your attention!

October 30th, 2024

Qiwei Shen

1st supervisor: Liangliang Nan

2nd supervisor: Jantien Stoter

Co-reader: Roderik Lindenbergh

Delegate: Daniëlle Groetelaers